



 Cite this: *RSC Adv.*, 2022, 12, 15261

# Light-responsive polyurethanes: classification of light-responsive moieties, light-responsive reactions, and their applications

 Ki Yan Lam,<sup>a</sup> Choy Sin Lee,<sup>b</sup> <sup>\*b</sup> Mallikarjuna Rao Pichika,<sup>bc</sup> Sit Foon Cheng<sup>d</sup> and Rachel Yie Hang Tan<sup>a</sup>

Stimuli responsiveness has been an attractive feature of smart material design, wherein the chemical and physical properties of the material can be varied in response to small environmental change. Polyurethane (PU), a widely used synthetic polymer can be upgraded into a light-responsive smart polymer by introducing a light-sensitive moiety into the polymer matrix. For instance, azobenzene, spiropyran, and coumarin result in reversible light-induced reactions, while *o*-nitrobenzyl can result in irreversible light-induced reactions. These variations of light-stimulus properties endow PU with wide ranges of physical, mechanical, and chemical changes upon exposure to different wavelengths of light. PU responsiveness has rarely been reviewed even though it is known to be one of the most versatile polymers with diverse ranges of applications in household, automotive, electronic, construction, medical, and biomedical industries. This review focuses on the classes of light-responsive moieties used in PU systems, their synthesis, and the response mechanism of light-responsive PU-based materials, which also include dual- or multi-responsive light-responsive PU systems. The advantages and limitations of light-responsive PU are reviewed and challenges in the development of light-responsive PU are discussed.

 Received 7th March 2022  
 Accepted 1st May 2022

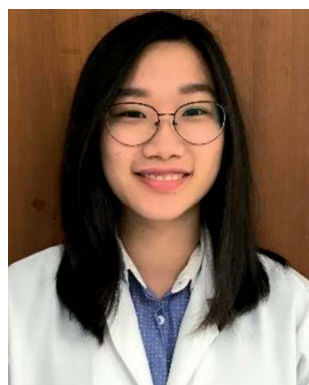
 DOI: 10.1039/d2ra01506d  
[rsc.li/rsc-advances](http://rsc.li/rsc-advances)

<sup>a</sup>School of Postgraduate, International Medical University, No. 126, Jalan Jalil Perkasa 19, Bukit Jalil, 57000 Kuala Lumpur, Malaysia. E-mail: choysin\_lee@imu.edu.my

<sup>b</sup>Department of Pharmaceutical Chemistry, School of Pharmacy, International Medical University, No. 126, Jalan Jalil Perkasa 19, Bukit Jalil, 57000 Kuala Lumpur, Malaysia

<sup>c</sup>Centre for Bioactive Molecules and Drug Delivery, Institute for Research, Development and Innovation, No. 126, Jalan Jalil Perkasa 19, Bukit Jalil, 57000 Kuala Lumpur, Malaysia

<sup>d</sup>Unit of Research on Lipids (URL), Department of Chemistry, Faculty of Science, University of Malaya, Kuala Lumpur 50603, Malaysia



*Ki Yan Lam received her Bachelor of Science (Hons) in Pharmaceutical Chemistry from the International Medical University, Malaysia in 2019. After her graduation, she pursued her M.Sc. by research in Medical and Health Sciences at the same university. Her research interests include the organic synthesis of novel stimulus-responsive polymers for functional applications such as drug*

*delivery, self-healing materials, smart coating, and other biomedical and bioengineering applications.*



*Choy Sin Lee (Ph.D.) is an associate professor at the Department of Pharmaceutical Chemistry, School of Pharmacy, International Medical University, Malaysia. She has 18 years of research experience and 13 years of teaching and supervision experience of research students. She has secured numerous national and international research grants and has filed 2 patents in Malaysia*

*and regional countries (Singapore, Thailand, Indonesia, and Vietnam). Her research interests are the organic synthesis of biocompatible and biodegradable polymeric materials from renewable resources and their applications in drug delivery and biomedical applications.*



## 1. Introduction

In recent years, a variety of stimulus-responsive polymers have been developed and their applications have been proposed. Stimulus-responsive polymers, also known as 'smart' polymers are gaining much attention from polymer industries due to their unique characteristics, demonstrating sensitive response to a slight change in stimulus factors such as light or ultraviolet (UV) light, temperature, pH variation, force, solvent, or reductant.<sup>1</sup> The activated polymers produce observable or detectable micro or nanoscale changes, such as morphology, molecular bond rearrangement, and molecular motion, which can induce changes in their macroscopic properties such as color, shape, and functionality.<sup>2</sup> Among the different stimuli that can be used

for activating smart polymers, light has several outstanding attractive features as it can be applied without contact, remotely, and provide spatial resolution to realize precise controllability, without time and space limitations, and tunable parameters such as source, wavelength, and intensity. Therefore, light-responsive polymers have attracted significant attention in recent years and attained great interest in engineering, biotechnology, biomedicine, and pharmaceutical applications.<sup>3,4</sup>

Light-responsive polymers can be enabled through the incorporation of light-sensitive moieties into the polymer networks. The light-sensitive moieties can respond to different wavelength ranges of light such as UV-C (100–280 nm), UV-B (280–315 nm), UV-A (315–400 nm), visible (400–780 nm), or near infrared (NIR) (780–2500 nm). Besides this, light-sensitive moieties undergo light-induced reversible and irreversible molecular structural changes, photothermal, crosslinking, as well as fluorescence up-conversion mechanisms. For instance, azobenzene and spiropyran perform reversible photoisomerization that can modify their polarity and/or conformation, while coumarin and anthracene undergo reversible photodimerization when exposed to light of an appropriate wavelength. The moieties with irreversible light-induced reactions include *o*-nitrobenzyl, acrylate monomer ion powder, and inorganic particles such as gold nanorods and carbon nanotubes. Polymers that respond to single stimulus, for instance, light responsiveness, may not satisfy certain requirements in practical application; thus, dual or multiple stimuli responsive polymers were studied as they respond to the respective stimuli, which could achieve the desired goals.

Table 1 summarizes the light-responsive groups used in polymers (excluded polyurethane) and their corresponding responsiveness and wavelength used for light irradiation. Due to the unique features of property changes in response to light, these polymer systems are emerging in wide ranges of



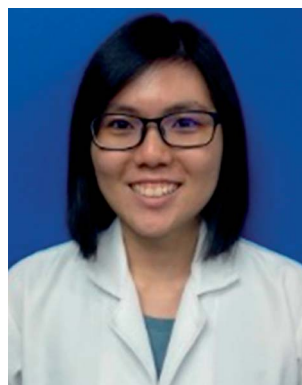
*Mallikarjuna Rao Pichika (Ph.D.) is a professor of Pharmaceutical Chemistry, School of Pharmacy, International Medical University, Malaysia. He is the Associate Dean (Research and Consultancy), School of Pharmacy, and Head of the Center of Excellence for Bioactive Molecules & Drug Delivery (BMDD), Institute for Research, Development and Innovation (IRDI), IMU. He has about 20 years of experience in*

*medicinal chemistry research. He is a Fellow of Royal Society of Chemistry (FRSC). His research interests include the design and development of new drug-like molecules and formulations for treating metabolic and infectious diseases. He has authored about 100 publications with an h-index of 21. The herbal formulations for cosmetic purposes and inflammatory conditions are in the market.*



*Sit-Foon Cheng (Ph.D.) is an associate professor at the Department of Chemistry, Faculty of Science, University of Malaya, where she has been a faculty member since 2008. To date, her research findings have resulted in five patents granted internationally. Her expertise is in the field of organic chemistry, more particularly, oleochemistry, as well as downstream and industrial applications. Her*

*research interests lie in the areas of natural resources and their potential for value-added products, through chemical modification, synthesis, extraction, characterization, and evaluation of food and non-food applications. She believes multidisciplinary research is the way forward for comprehensive insights into scientific problems and issues.*



*Rachel Yie Hang Tan received her Bachelor of Science (Hons) in Pharmaceutical Chemistry from the International Medical University, Kuala Lumpur, Malaysia, in 2019. She continued her postgraduate by research studies in Medical and Health Sciences at International Medical University. Her research interests include the synthesis of polymeric materials from renewable resources and*

*exploring their applications in drug delivery systems and biomedical fields.*



**Table 1** Light-responsive groups used in polymers (excluded polyurethane) and their corresponding responsiveness and wavelength used for light irradiation (published in the year of 2019–2020)

Polymer	Light sensitive moiety	Light-responsive region [nm]			Responsiveness	Application	Ref.
		UV	Vis	NIR			
<b>(a) Medical and biomedical applications</b>							
Polyester (PE)	Graphene quantum dots	365	400–700		Light	Drug delivery system	21
Poly[oligo(ethylene glycol)methylether methacrylate]	1-Pyrenemethyl methacrylate	365			Light	Drug delivery system	22
Poly( $\epsilon$ -caprolactone) (PCL)	Indocyanine green			808	Light	Drug delivery system	23
Poly(ethyleneimine)	Cinnamic acid-UV gold nanoparticle-NIR	365		808	Light	Drug delivery system	24
Poly(2-isopropyl-2-oxazoline)	1,3,3-Trimethylindolino-6'-nitrobenzopyrrolospiran	365	440		Thermo Light	Drug delivery system	25
Polyacrylamide	Azobenzene acrylamide	365	450		Thermo Light	Drug delivery system	26
					Light	Catalyst carriers	
Poly((7-(4-vinyl-benzyloxy)-4-methylcoumarin)- <i>co</i> -acrylic acid)- <i>b</i> -poly((2-(dimethylamino)ethyl methacrylate)- <i>co</i> -styrene) (P(VBMC- <i>co</i> -AA)- <i>b</i> -P(DMAEMA- <i>co</i> -St))	7-(4-Vinyl-benzyloxy)-4-methylcoumarin	254, 365			pH Light	Drug delivery system	27
Polyethylene glycol (PEG)/PCL	Host-guest interaction between $\beta$ -CD and azobenzene	365			Glutathione Light	Drug delivery system	28
Poly(methyl methacrylate) (PMMA)	9-Anthracenecarboxylic acid	254 365			CO <sub>2</sub> Light	Drug delivery system	29
	1,3-Dihydro-1,3,3-trimethylspiro[2 <i>H</i> -indole-2,3'-[3 <i>H</i> ]naphth[2,1- <i>b</i> ][1,4]oxazine]	254			Light	Smart sensor	30
Tetraphenylethylene-based covalent organic polymer	Phosphor	370			Fe <sup>3+</sup> Light	Biosensors of Fe <sup>3+</sup> White-light emitting diodes	31
Poly( <i>N</i> -isopropylacrylamide) (PNIPAM)/cysteamine	Gold		405 462 520 635	785	Thermo Light	Gas sensors	32
Polycarbonate	Photosensitizer 5,10,15,20-tetrakis( <i>m</i> -hydroxyphenyl)chlorin	365			Light	Photodynamic therapy	33
Poly( <i>N</i> -vinylpyrrolidone)	Crown- and phosphoryl-containing metal phthalocyanines		670		Light	Photodynamic therapy	34
Poly( <i>D,L</i> -lactic- <i>co</i> -glycolic acid)	Gold nanorods			808	Light	Photothermal therapy	35
PEG	Pd(II)			820, 1064	Light	Photoacoustic (PA) imaging-guided photothermal therapy (PTT)	36
Thiolated cyclo(Arg-Gly-Asp-D-Phe-Lys(mpa)) peptide	Conjugated polymers			808	Thermo Light	Photothermal therapy	37
PEG-PPG copolymer	Photosensitive porphyrin zirconium metal		488		Redox Light	Chemo-photodynamic therapy	38
Conjugated 1,2-distearoyl- <i>sn</i> -glycero-3-phosphoethanolamine- <i>N</i> -[carboxy(polyethylene-glycol)-2000]-lanreotide	Copper sulfide nanoparticles			808	Light	Chemo-photothermal therapy	39
Fluorinated polyethylenimine	Semiconducting polymer brush			808	Light	Genome-editing-based precise gene therapy	40
Polystyrene- <i>b</i> -poly( <i>N</i> -isopropylacrylamide- <i>co</i> -acrylic acid)	Diketopyrrolopyrrole-based semiconducting polymer poly[{2,5-bis(2-hexyldecyl)-2,3,5,6-tetrahydro-3,6-dioxopyrrolo[3,4- <i>c</i> ]pyrrole-1,4-diyl}- <i>alt</i> -{[2,2':5',2''-terthiophene]-5,5''-diyl}]			785	pH Thermo Light	Chemo-photothermal therapy	41



Table 1 (Contd.)

Polymer	Light sensitive moiety	Light-responsive region [nm]			Responsiveness	Application	Ref.
		UV	Vis	NIR			
Polyimide	2,2'-Azobisisobutyronitrile	375	530		Thermo Light	—	42
Cross-linked polyethylene glycol diacrylate	Oligo(ethylene glycol)-modified W <sub>18</sub> O <sub>49</sub> nanowires	365		808 980	Light	Artificial muscles and minimally invasive surgery	43
Poly(L-lactide)-poly(ε-caprolactone) copolymer	7-Hydroxy-4-methylcoumarin	254 365			Thermo Light	Medicine Textile	44
PNIPAM/clay	Polydopamine nanoparticles			808	Thermo Light	Soft robots Soft intelligent robots Wearable devices	45
Poly(2-(2-methoxyethoxy)ethyl methacrylate) and poly(N-[4-(4-nitrophenyl)azo]phenyl acrylamide) mixed polymer brushes	(N-[4-(4-Nitrophenyl)azo]phenyl acrylamide)	365	450		Thermo Light	Cell sheet preparation and detachment state	46
L-Phenylalanine benzyl ester	4-[(4-methacryloyloxy)phenylazo] benzoic acid	365	400–700		Light	Molecular imprinting	47
Polyethylene/polylactic acid	Azobenzene	360			Light	Antimicrobial active packaging Drug delivery Agriculture Household and cosmetics	48
<b>(b) Engineering applications</b>							
Polyimide	4-Amino-1,1'-azobenzene-3,4'-disulfonic acid monosodium salt, (C <sub>12</sub> H <sub>10</sub> N <sub>3</sub> NaO <sub>6</sub> S <sub>2</sub> ) UV curing agent (Trade name: LS-2211)	365			Light	Coated optical fiber	49
PEG	Benzophenone	365			Light	Waterborne UV coatings, inks and adhesives	50
Latexes	2-(4-(4-Butylphenyl)diazanylphenoxy) ethyltrimethylammonium bromide	365	460		Thermo Light	Reversible destabilization Paints	51
Polydimethylsiloxane	Zirconia nanoparticles	365			Thermo Light	Anti-reflective coatings Gas separation	52
PMMA	1,3-Dihydro-1,3,3-trimethylspiro[2H-indole-2,3'-[3H]naphth[2,1-b][1,4]oxazine]	254			Light Light	Smart sensor	30
Poly(3-hexylthiophene)graphene	Poly(3-hexylthiophene)-graphene		532		Light	Smart sensors telecommunication	53
Cellulose acetate	Azobenzene	254			Light	Optical switches for liquid crystalline alignment	54
PE	4,4-Dihydroxyazobenzene	365	550		Thermo Light	Actuators to electro-optical devices	55
Polystyrene	Carbon dots	365			Light	White-light-emitting devices	56
Poly(ethylene-co-vinyl acetate)	Graphene			—	Thermo Light	Shape memory actuator	57
Liquid crystalline elastomers network	Azobenzene		532		Light	Shape memory polymer	58
Poly(allyl methacrylate)	Asymmetric divinyl monomers	254			Light	Crosslinked polymer	59
Benzene-1,4-diboronic acid with the 1,3-diol polymer	Azobenzene	365	435		Light	Crosslinked polymer	60



Table 1 (Contd.)

Polymer	Light sensitive moiety	Light-responsive region [nm]			Responsiveness	Application	Ref.
		UV	Vis	NIR			
Poly[(Z)- $\omega$ -(4-(1-cyano-2-(4-cyanophenyl)vinyl)phenoxy)alkyl methacrylate]	$\alpha$ -Cyanostilbene	254	365		Thermo Light	Luminescent liquid crystals	61
$\alpha$ -CD-bearing telechelic poly(2-isopropyl-2-oxazoline)	Azobenzene-bearing penta(ethylene glycol)	254	365		Thermo Light	Multi-functional thermo- and photo-sensitive materials	62
Polymeric O and N co-linked carbon nitride framework	Carbon dots		450		Light	Pollutant degradation environmental remediation	63
Poly(ethylene- <i>co</i> -butylene)	Isophthalic acid-pyridine	320– 390			Thermo Light	Debonding-on-demand applications	64
1,4-(Bis-chlorotetrafluoro- $\lambda$ 6-sulfanyl) benzene with 1,4-diethynylbenzene	Hypervalent fluorinated sulfur	200– 450			Light	Micro-electronic lithographic	65
Poly(dimethylsiloxane)	1-(4-(Hex-5-enyloxy)phenyl)-2-phenyldiazene	365			Thermo Light	Logic gate	66
Poly(3-hexylthiophene)	Poly(3-hexylthiophene)			808	Light	Liquid marble stabilizer	67

applications in drug and gene delivery, photothermal therapy, photodynamic therapy, tissue engineering, and biosensors under UV or NIR light. Their applications are in engineering areas are such as logic gates, white light emitting diodes, and UV-curing technique for coating and paints. These polymers are responsive to UV and/or Vis and/or NIR light.

On the other hand, polyurethane (PU) is a synthetic polymer that is majorly produced by reacting polyisocyanates and polyhydroxyl compounds, also known as polyols. PUs with different macromolecular structures are specified for diverse applications in engineering, automotive, military, medical, and biomedical products. The reactions of different types and ratios of polyisocyanates and polyols are able to customize the physical, chemical, mechanical, and thermal properties of the final products. This is because of PU is formed by two different segments, *i.e.*, hard and soft segments in the polymer matrices. The hard segment is mainly structured by the urethane linkages between the isocyanate and the chain extender, whereas the soft segment is confirmed by the polyol or diol groups,<sup>5</sup> making it a versatile polymeric material with wide ranges of specifications and properties. The highly tunable properties of PU also enable its incorporation with different kind of photochromic groups without compromising its physical and mechanical properties, which is beneficial for stimuli responsiveness as a smart material (Fig. 1).

Light-responsive PUs are promising candidates for engineering applications such as smart coating for textiles and optical devices,<sup>6,7</sup> UV-curable PU in flame retardant<sup>8</sup> and coatings,<sup>9</sup> piezoresistive<sup>10</sup> or photo-thermal sensors,<sup>11</sup> as well as robotic fingers with shape memory properties.<sup>12</sup> The excellent physical and mechanical properties as well as biocompatibility of PUs<sup>13</sup> with the additional advantages of light responsiveness

have further widened the applications of PUs as a smart material for medical and biomedical applications. For instance, light-responsive PUs have been used as biomimetic actuators with self-healing properties,<sup>14</sup> implantable devices,<sup>15</sup> or skin care patches<sup>16</sup> with shape memory effect, artificial skin for tissue engineering,<sup>17</sup> and drug carriers for controlled drug delivery systems,<sup>18–20</sup> which all arise from the tunable properties of PUs and the highly controllable properties during light-induced reactions. A summary of the currently available studies involving light-responsive moieties and responsiveness of these light-responsive PUs is presented in Table 2.

To the best of our knowledge, there is no reported review article on the topic of light-responsive PUs, especially in medical and biomedical areas. The main aim of this review is to summarize the potential light-responsive polyurethane-based materials that have been used in medical and biomedical engineering and wastewater treatment applications. After the introduction of light responsiveness PUs, Section 2 will summarize the recent reports on the synthesis and design of PUs, which show potential for developing single or multifunctional stimuli responsiveness to light and other factors. The chemical, physical, mechanical, and thermal properties of the PUs triggered by light stimuli are also included in this review. Finally, the key points have been highlighted for development and challenges in future research.

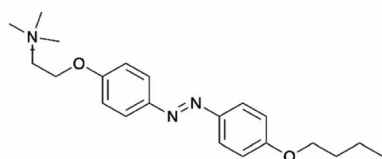
## 2. Light-responsive polyurethane

Table 2 summarizes the light-responsive groups used in polyurethane and their corresponding responsiveness and wavelength used for light irradiation. The light-responsive PUs reported here have been discussed in the following section.

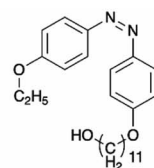


## Azobenzene and derivatives

(a)

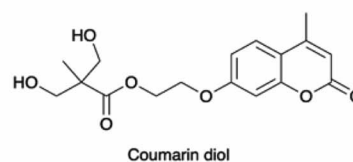


(b)



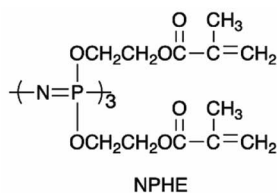
## Coumarin derivatives

(c)



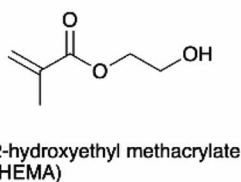
## Inorganic particle

(d)

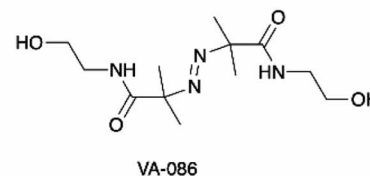


## Acrylate with photoinitiator

(e)

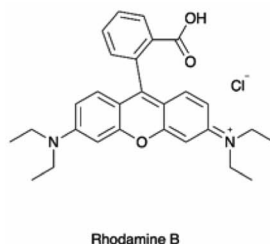


(f)



## Fluorescent

(g)



## Dithiocarbamate iniferter

(h)

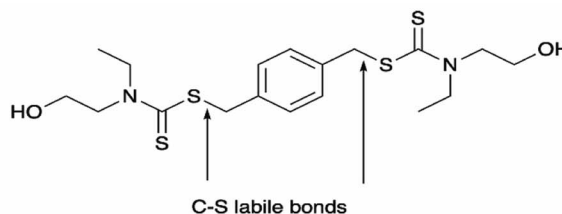


Fig. 1 (a–h) The chemical structure of photosensitive moieties.

Section 2 presents the reversible light-induced isomerization and dimerization reaction, irreversible light-induced cleavable reaction, and light-induced crosslinking reactions.

### 2.1. Light-induced isomerization reaction

Light-induced isomerization or photoisomerization is a molecular behavior in which structural changes as the *trans-cis* isomerization of molecules with a double bond is caused by photoexcitation. For certain molecules, this process is reversible and repeatable, making these photoisomerization groups more attractive in designing polymers with a broad range of applications. Dichloroethylene is an example of a molecule for which a light-induced irreversible isomerization is known.<sup>86</sup> By considering biomedical applications, the irreversibility of isomerization prevents a non-invasive subcutaneous application or the easy recovery of the cells when hydrogels are used as scaffolds for cell housing. In this review, only reversible photoisomerization will be discussed. The reversible photoisomerization groups that have been incorporated in PU are azobenzene (AZO) (Fig. 2a) and spiropyran (SP) (Fig. 2b). The light-induced transitions in azobenzene groups caused changes

in both the isomerization structures as well as the polarity of the compound. The linear *trans*-isomer is non-polar, while the bent *cis*-isomer is more polar due to the change in the symmetry. For the *cis*-isomer, the benzene rings are on the same side of the molecule; thus, the atoms experience different polarity. Hence, the *cis*-isomer is a polar molecule. The AZO-based PUs can be transformed upon UV light irradiation (365 nm)<sup>6,18,73–75</sup> from *trans* to *cis*-azobenzene and reversibly from *cis* to *trans* when exposed to visible light (450 nm to 530 nm)<sup>11,68–72</sup> or heat for reversible photoisomerization. Besides, colorless SP is one of the mechanophores that can be ring-opened in response to UV at 365 nm or applied stress and thus convert to a purple merocyanine (MC) form. Photoisomerization is one of the simplest light-induced reactions that can be applied in polymers and include *trans-cis* isomerization and heterocyclic cleavage.

The single and dual responsiveness of AZO-based PU with light-induced *trans-cis* isomerization and SP-based PU with heterocyclic cleavage reaction are discussed in the following sections.

**2.1.1. Azobenzene-based polyurethanes.** Azobenzene is one of the most widely used photochromic compounds in light-



Table 2 Light-responsive groups used in polyurethane and their corresponding responsiveness and wavelength used for light irradiation

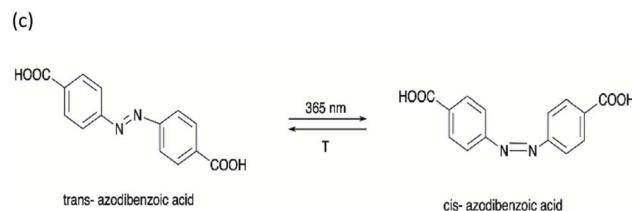
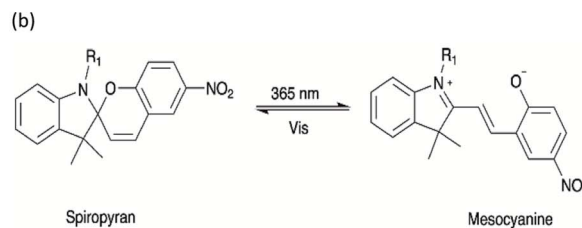
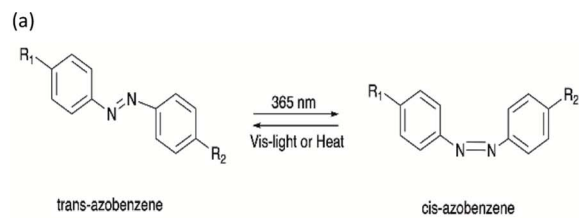
Light-responsive group		Responsiveness				Wavelength used for light irradiation [nm]				
Classification	Light-responsive moiety	Light	Thermal	pH	Forces	Reduction	UV	Vis	NIR	Ref.
Azobenzene and derivatives	Dihydroxyazobenzene (DHAB)	—	—				320–500			68
	4,4'-Diaminoazobenzene (DAB)	—					385	440		69
	4-Butoxy-4'-(trimethylaminoethoxy) azobenzene (BTAEazo)	—					360	450		70
	Azobenzene, 4-cyano-4'-pentyloxyazobenzene (5CAZ) and upconversion nanoparticles	—	—				365	530	808	71
	Pentaerythritol [SCLCPU(AZO)-N]	—	—					450, 550		72
	4-Octyldecyloxybenzoic acid (TABA)	—	—				365	460		11
	4'-Ethoxy-4-(11-hydroxyundecyloxy)-azobenzene (EHAB) and graphene oxide (GO)	—	—				—			14
	4-(4-Oxyalkyl chain carbonyl)azodibenzoic acid (Azo11)	—	—				365			73
	4,4-Azodibenzoic acid (Azoa)	—	—				365			74
	N,N-Dihydroxyethylazobenzene	—		—			365			6
Spiropyran Coumarin derivatives	2,20-(4-((4-Ethylphenyl)diazanyl)phenylazanediyldiethanol (EDPD)	—		—			365			75
	Azobenzene and 3,3'-disulfanediyldipropene-1,2-diol (DSO)	—			—		365			18
	Di-hydroxylspiropyran	—			—		365			7
	7-(Hydroxyethoxy)-4-methylcoumarin (HMEC)	—					254,			76
							365			
	7-Bis(2-hydroxyethoxy)-4-methylcoumarin (DHEMC)	—					254,			77
							365			
	Coumarin diol	—					254,			78
							365			
	4-Methyl-7-((4-oxopentyl)oxy)-2H-chromen-2-one (OMC) and hydrazone bond	—		—			365			19
Anthracene	3-(N,N-Bis (2-hydroxyethyl)amine)propionic acid-9-anthracenemethanol ester (BHPAE)	—	—				365			79
Nitrobenzyl derivative	<i>o</i> -Nitrobenzyl ( <i>o</i> -NB)	—					365			20
Inorganic particles	Multiwalled carbon nanotubes, NC7000™	—					395			10
	Phosphorus derivative (phosphazene)	—					365			8
Acrylate with photoinitiator	2,2'-Azobis[2-methyl-N-(2-hydroxyethyl)propionamide] (tradename: VA-086)	—	—				365			80
	Irgacure 184 and Irgacure 819	—					365			81
	Darocur 1173	—					365			9
	Darocur 4265	—					365			82
Negative ion	Ag <sub>3</sub> PO <sub>4</sub> @AgBr	—						> 420		83
Fluorescent	Rhodamine B (RhB)	—	—				365			84
Other	Dithiocarbamate iniferter	—					365			85

responsive polymers for reversible *trans-cis* photoisomerization. Li *et al.* presented a thermoplastic PU-based photomechanical elastomer (PME) with light-responsive and self-healing properties.<sup>69</sup> PME was synthesized by reacting toluene-2,4-diisocyanate (TDI) and poly(propylene glycol) (PPG) to produce a PU prepolymer, followed by reaction with the PU prepolymer with 4,4'-methylenedianiline (MDA) and DAB (Scheme 1). The PME produced was proven for its light-responsive properties that were comparable to light-responsive DAB-based liquid crystal elastomers, which required complex molecular design and specialized equipment to obtain the liquid crystal mesogens. The PME exhibited bending motion when it was irradiated with UV light at 385 nm and was restored to its original shape after exposure to visible light at 440 nm. The DAB chromophores in the polymer

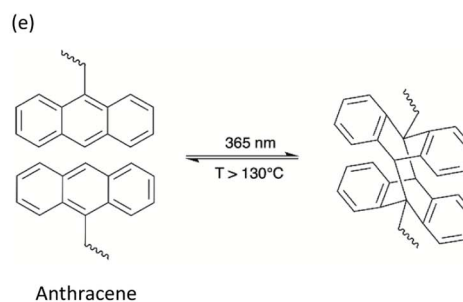
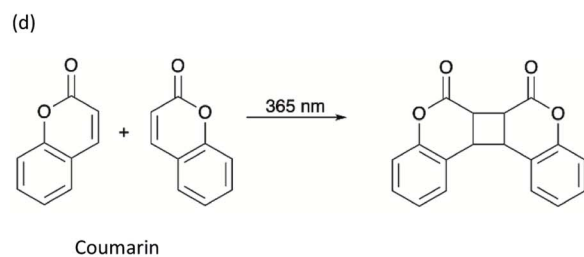
matrices appear in *trans*-configuration (thermodynamically more stable form) when the polymer was kept in the dark at room temperature. When irradiated at UV light ( $\lambda = 385$  nm), the *trans*-DAB transformed into the *cis*-configuration. On the other hand, the curled up PME was able to return to its original form when irradiated with visible light (440 nm) due to *cis*-DAB transforming back to the *trans*-configuration, demonstrating its light-induced isomerization behavior. The PME also demonstrated self-healing properties where the PME film was cut uniaxially into two pieces and brought the freshly cut edges into contact for 5 min at room temperature. The PME film was able to stretch to 100% strain without breaking (Fig. 3a). The author proposed that the elasticity and autonomous self-healing properties of the PME resulted in the double network of dynamic hydrogen bonding of ureas and urethanes in the



## Reversible photoisomerization



## Photodimerization



## Light-induced crosslinking

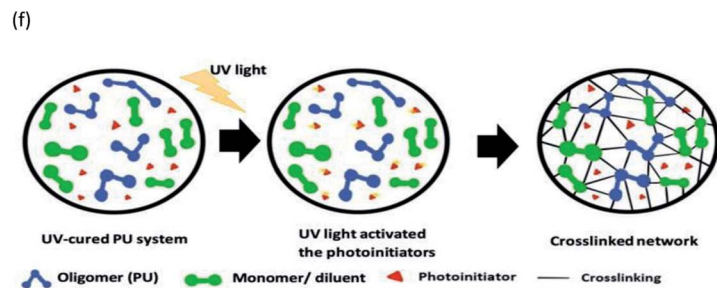


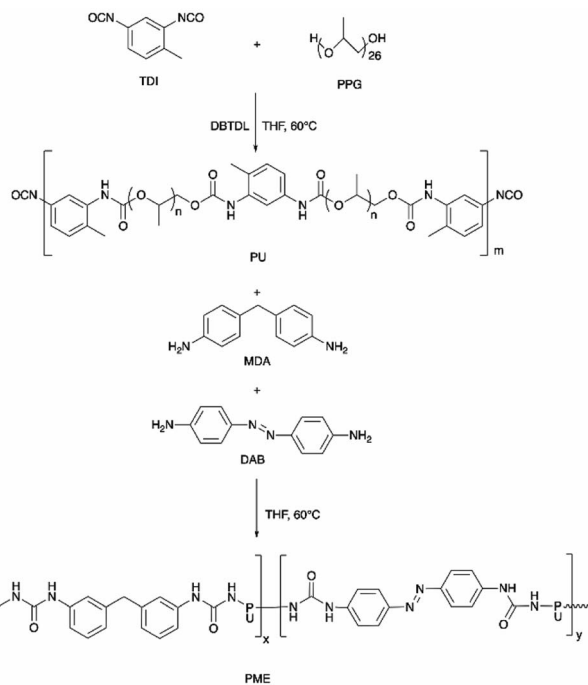
Fig. 2 (a–f) The light-induced reactions.

polymer matrices.<sup>69,87,88</sup> The urea groups formed by the reaction of diamines (MDA and DAB) with isocyanate offer bidentate sites for strong hydrogen bonding between N–H and C=O, while the urethane groups were obtained by the reaction of polyol, PEG, and isocyanates that provide one site of weak monodentate hydrogen bonding linkage (Fig. 3b). In addition, hydrogen bonding can be established between the bidentate urea groups and the monodentate urethane groups.<sup>69,89</sup> The strong hydrogen bonding gives elasticity that ensures full recovery from large strains, while the weak hydrogen bonding leads to energy dissipation after breaking and reforming.<sup>69,90</sup> The PU system was proposed to serve for the construction of light-responsive soft robotic gripper.

Chen *et al.* developed a dye-bonded blocked waterborne polyurethane (BWPU) as a coloring agent and light-responsive

cationic surfactant BTAEazo in a green cotton coloring process for cotton fabrics.<sup>70</sup> The PU foam was synthesized by reacting isophorone diisocyanate (IPDI) and PEG, and subsequently coated with a BTAEazo containing dye liquid as the surfactant to prepare the dye-bonded BWPU (Fig. 4). The synthesized BTAEazo showed light sensitivity photoisomerization capability under UV or visible light irradiation. The dye-bonded BWPU foam was applied onto cotton fabrics using a control coater to dye the fabrics. The residual foam collected after the dyeing process was exposed to UV light ( $\lambda = 360\text{ nm}$ ) so that the BWPU foam ruptured and was recycled in the liquid form. The recycled coating liquid was then irradiated with visible light ( $\lambda = 450\text{ nm}$ ) to regain the foam stabilized capability to be reused in the dyeing processes. BTAEazo-PU was reported to be light-sensitive after 20 cycles of repetitive





Scheme 1 The reaction scheme for the synthesis of the photo-mechanical elastomer PME.

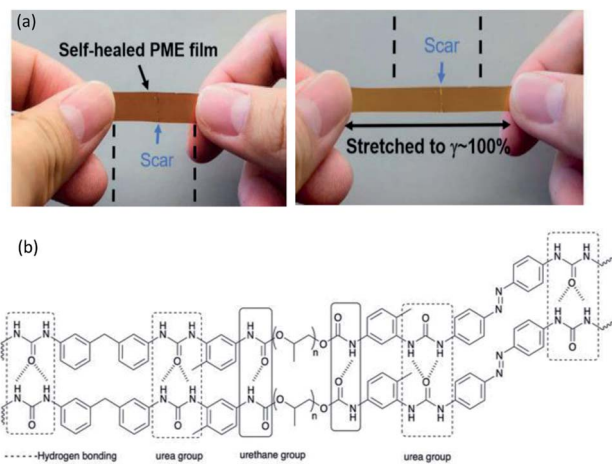


Fig. 3 (a) The PME film was cut into two pieces and held together for 5 min at 23 °C. The film can then be stretched to 100% strain without breakage. Reproduced with permission.<sup>69</sup> Copyright 2019, John Wiley and Sons, and (b) the H-bonding in the PU structure of the thermo-plastic PU-based PME with light-responsive and self-healing properties. The hashed bonds show the H-bonding.

photoisomerization, which indicated that the addition of the dye did not affect the foamability of BTAEAzo in the foaming process under light exposure.

**2.1.2. Azobenzene-based polyurethane with dual stimuli-responsiveness.** Some of the AZO-based PUs demonstrate dual light- and thermo-responsiveness when the azobenzene acid and amide derivative exhibit light-responsive deformation under UV light exposure and shape recovery upon visible light

exposure or heating. This typical dual light- and thermo-responsive PU is being used as a shape memory PU for tissue engineering applications.<sup>11,72</sup> As compared to pH or redox stimulus, thermal and light responsiveness have a higher degree of freedom due to the precise control over the temporal and spatial localization of the responsiveness as well as lower the limitation of specific physiological environment of the targets. The temperature variation can be adjusted through light illumination or thermal heating, which can be applied artificially rather than exploiting particular conditions of the targeted organs or tissues.

Meanwhile, dual light- and pH-responsive PUs containing AZO have potential application in sensors for the purpose of monitoring the environmental changes.<sup>6,74,91</sup> Considering the biomedical field as an example, the intracellular pH plays an important role in cell, tissue, and enzymatic activities. Monitoring the pH changes and gradients are crucial to investigate cellular internalization pathways and diagnose certain diseases. With the addition of pH response, the light-responsive PU could be used as a biosensor to specifically monitor pathophysiological conditions of the targets.

When azobenzene is incorporated with other functional groups such as disulfide with reductant properties, the azobenzene PU is used in the drug delivery system.<sup>18</sup> The synergistic effect of the light-responsive azobenzene moiety and the reductant-responsive disulfide in the PU hydrogel, which improved the drug release profile of the hydrophobic drug.

**2.1.3. Light- and thermo-responsive polyurethane containing azobenzene.** Fang *et al.* reported on the production of a light-responsive PU containing AZO by reacting isophorone diisocyanate (IPDI) and polycarbonate diols (PCDL,  $M_w = 2000 \text{ g mol}^{-1}$ ), followed by reaction with the synthesized DHAB<sup>68,92</sup> as the chain extender. The AZO-PU exhibited UV light-responsive deformation capability and thermally-induced shape memory effect (Fig. 5). The PU-containing AZO was subsequently stacked up with poly(ethylene-co-vinyl acetate) (EVA) composites containing photothermal fillers using a silicon adhesive sealant. The polymer exhibited UV light-responsive deformation capability owing to the functional monomer DHAB chain extender with short wavelength UV light absorption capability in the range of 320–600 nm, which underwent *trans-cis* photoisomerization upon UV irradiation. The bending deformation of the polymer sheet was reported to be due to UV light penetrating a few micrometers on the AZO-based PU film surface, hence causing the *trans-cis* photoisomerization on the azobenzene moieties lying close to the upper surface of the PU. The reversible mechanism of the photoisomerization of azobenzene from *cis* to *trans* upon visible light irradiation was not reported. The shape recovery of the polymer was reported to be aided by the EVA composite film containing the photothermal filler such as gold nanoparticles (AuNPs), Nd(TTA)<sub>3</sub>Phen, Yb(TTA)<sub>3</sub>Phen, and Sm(TTA)<sub>3</sub>Phen, in which these fillers were responsive toward visible (250 nm) and NIR (808–1064 nm) light. Besides, the AZO-based PU also demonstrated thermally-induced shape memory effect. The AZO-based PU film was deformed at 80 °C to 100% and subsequently cooled down to room temperature with a shape fixity ratio of about 94% due to the redevelopment of



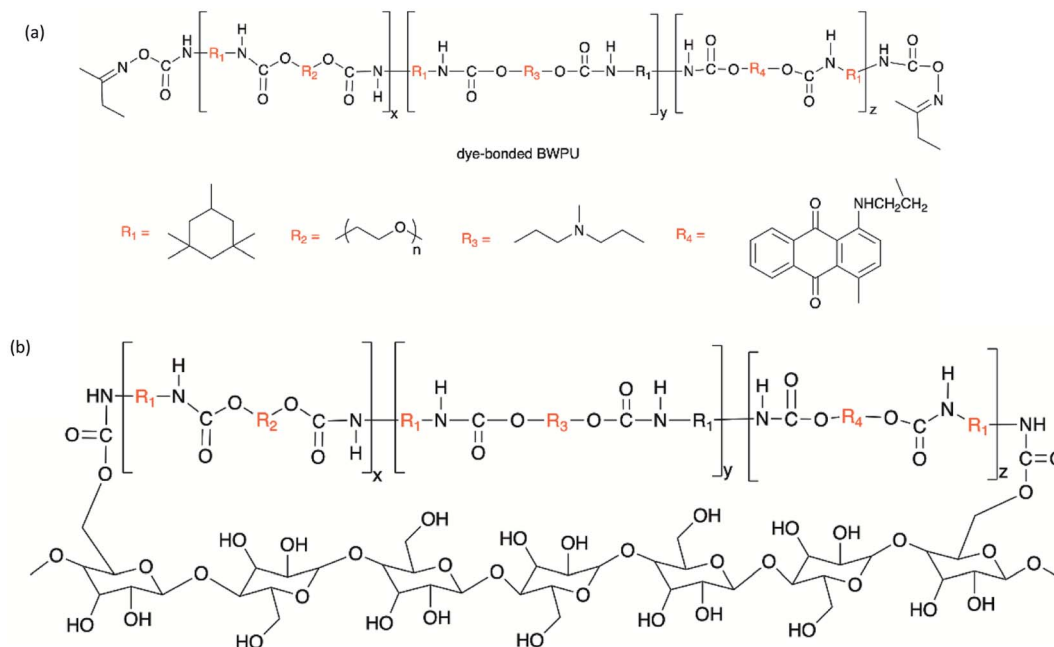


Fig. 4 The chemical structure (a) dye-bonded BWPU and (b) dye-bonded BWPU-coated cotton fabric.

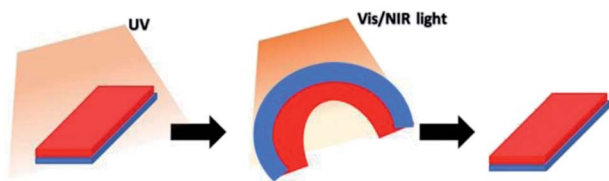


Fig. 5 The schematic illustration of shape memory of the bilayer film consisting of AZO-PU and EVA composites upon UV/Vis/NIR light irradiation (red: AZO-based PU layer and blue: EVA composite with photothermal filler layer).

the glassy state of the partial soft segment. The recovery ratio was approximately 60% when the PU film was heated at 100 °C as the hard segments with high  $T_g$  were considered to serve as physical net points.

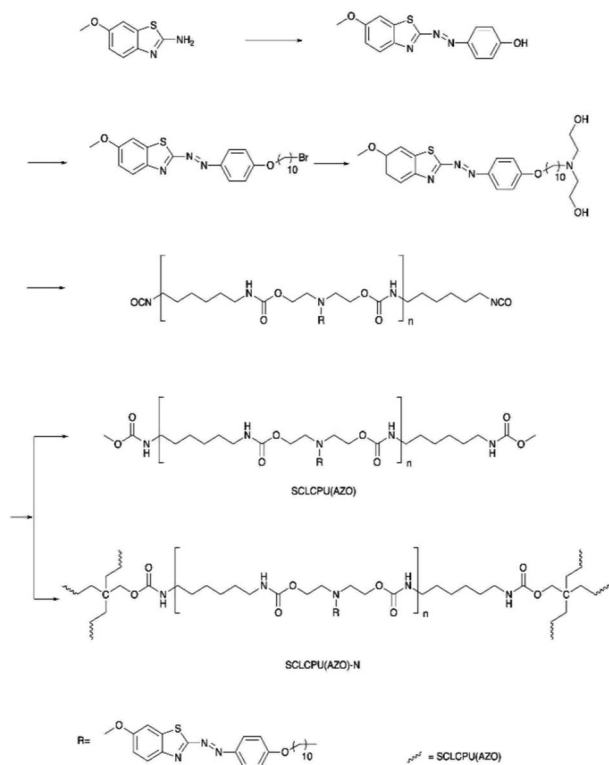
Wen *et al.* reported a dual light- and thermo-responsive PU, side-chain liquid crystalline polyurethane networks based on the pendant azobenzene group [SCLCPU(AZO)-N]. SCLCPU(AZO)-N was synthesized by reacting the functional azobenzene diol monomer (derived from 2-amino-6-methoxybenzothiazole) with 1,6-hexamethylene diisocyanate (HDI) to form the linear SCLCPU(AZO) precursor and subsequently crosslinked the SCLCPU(AZO) precursor with pentaerythritol (Scheme 2).<sup>72</sup> The bending and unbending of the SCLCPU(AZO)-N films were due to the *trans-cis* photoisomerization of azobenzene by irradiation with visible light at 450 nm and 550 nm. When the SCLCPU(AZO)-N film was exposed to visible light ( $\lambda = 450$  nm), the sample underwent *trans* to *cis* isomerization and SCLCPU(AZO)-N returned to the initial state from *cis* to *trans* at an irradiation wavelength of 550 nm; SCLCPU(AZO)-N displayed a triple shape memory effect

by demonstrating two independent glass transition temperature ( $T_g$ ) and a clearing point ( $T_{ci}$ ) with a temperature difference of more than 40 °C, making it a thermo-responsive PU material. The architecture of the SCLCPU(AZO)-N networks giving the triple shape memory effect could be adjusted by the molecular weight of the SCLCPU(AZO) precursors used in the reactions.

Zhou *et al.* reported on the fabrication of PU-GO, PU-EHAB film, and PU-EHAB-GO films.<sup>14</sup> The PU employed was a PCL-based commercial shape memory PU (SMPU) (KH330, Yuntaihaina Environmental Protection Technology Co., Ltd) with thermal responsive properties. The PU composite film was fabricated by casting the SMPU, GO, and/or EHAB solution in DMF on a glass slide and left to dry to obtain the PU-GO, PU-EHAB, and PU-EHAB-GO films. EHAB and GO acted as photoharvesters for UV and NIR light, and their light-responsiveness was transferred to the host SMP films. EHAB was proven for its *trans-cis* photoisomerization that was triggered by UV light. Upon exposure to UV light (source: HTLD-4 II Shenzhen Height-LED Opto-electronic Tech Co., Ltd, wavelength: not reported), the mechanically stretched PU-EHAB-GO films bent toward the light sources as the light-induced photoisomerization occurred on the film surface. On the other hand, GO with photothermal effect with good absorption toward NIR light (source: MDL-H Changchun New Industries Optoelectronics Technology Co., Ltd, wavelength: not reported) and the bent PU-EHAB-GO film also recovered its initial shape after NIR light irradiation (Fig. 6b). Besides, the stretched PU-GO-EHAB film was also nearly recovered to its original shape by heating at 85 °C. The PU-EHAB-GO composites were reported for their potential application in biomimetic actuation.

Zhang *et al.* developed a UV-Vis-NIR photo-activated PU composites *via* the incorporation of 5CAZ and up-conversion





Scheme 2 The reaction scheme for the synthesis of SCLCPU(AZO) and SCLCPU(AZO)-N.

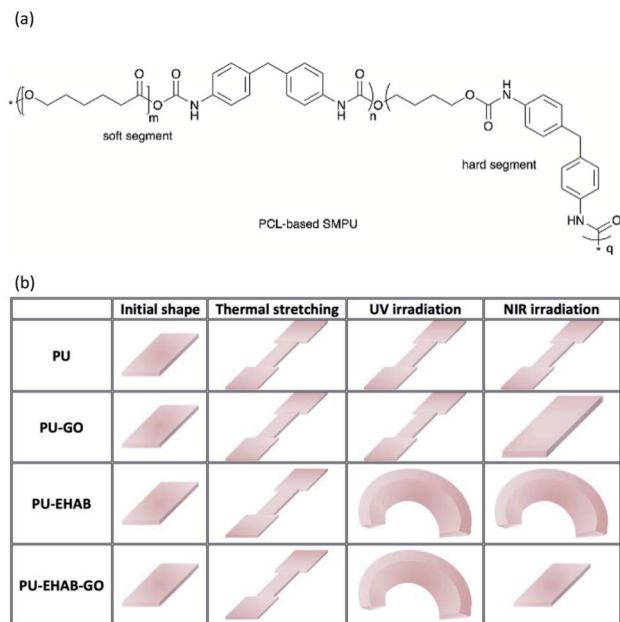


Fig. 6 The chemical structure of (a) EHAB and (b) PCL-based SPU and (c) illustration of the light-responsive triple shape-memory effect (SME) in thermal stretching, as well as UV and NIR light irradiation.

nanoparticles (UCNPs) into a commercial thermo-responsive shape memory polyurethane (SMPU) ( $M_n = 1.2 \times 10^5 \text{ g mol}^{-1}$ ,  $PDI = 2.25$ ).<sup>71</sup> The UCNPs were able to convert low energy light

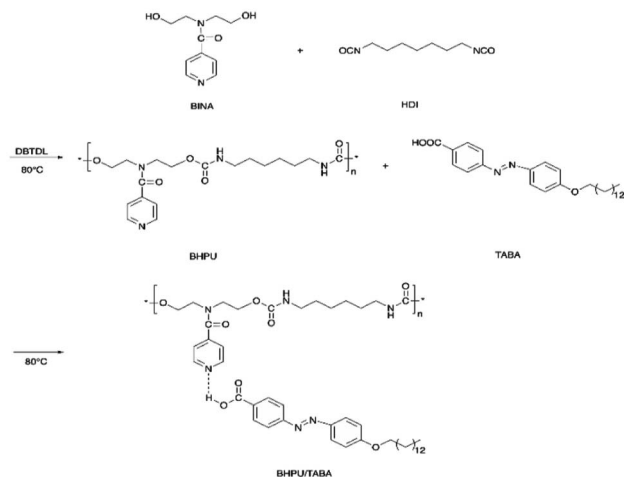
such as NIR light into a high energy light; thus, a long wavelength (NIR light) light-responsive polymer also can be obtained by introducing UCNPs into the polymer matrix. 5CAZ served as a light sensitive group and underwent *trans-cis* photoisomerization under UV light (365 nm) and visible light (530 nm) exposure. The synthesized UCNPs were used to convert NIR light at 808 nm into green fluorescence by continuous photon absorption. The 5CAZ/UCNP/SMPU film formed a bilayer structure and the concentration of 5CAZ was higher at the upper layer due to small surface energy. The authors applied mechanical stretching on the 5CAZ/UCNP/SMPU film before performing light irradiation in order to get a more ordered distribution of the 5CAZ content. When the surface of the stretched 5CAZ/UCNP/SMPU film exposed to UV/Vis/NIR light, the volume contraction of the upper layer was higher than the lower layer, which results in film bending toward the light source. The 5CAZ/UCNP/SMPU film exhibited triple shape memory effects as the stretched film was bent upward upon UV/visible light/NIR light irradiation. The film was able to recover to its initial shape (before stretching) upon heating at 90 °C. It was reported that the NIR light could not induce the azo-moieties of 5CAZ to isomerize from *trans* to *cis* and up-conversion fluorescence without the presence of UCNPs (Fig. 7). The assembled PU film was prepared as a biomimetic finger-like product, which demonstrated a larger bending degree upon UV irradiation as compared to NIR irradiation.

Li *et al.* also reported a dual light-and thermo-responsive staging supramolecular shape memory PU complexes formed by the pyridine-based PUs and azobenzene-based mesogens.<sup>11</sup> The pyridine-based SMPU (BHPU) complexes obtained by reacting HDI and *N,N*-bis(2-hydroxyethyl) isonicotinamide (BINA) were first synthesized by reacting *N,N*-bis(2-hydroxyethyl) isonicotinamide (BINA) with HDI. Subsequently, BHPUs were added with azobenzene mesogens TABA to form the supramolecular BHPU/TABA complex *via* hydrogen bonds between the pyridine rings and carboxyl groups of TABA mesogens (Scheme 3). The addition of TABA increased the glass transition temperature, thermal stability, and storage modulus while promoting the microphase separation in the new complexes. These physical, thermal, and structural changes (microphase separation) contributed to the multi-shape memory and thermal responsive properties of the PU. Under the thermal-induced shape memory effect, the TABA formed intermolecular hydrogen bonds with the pyridine of the PU



Fig. 7 Schematic illustration of the bending mechanisms for 5CAZ/UCNP/SMPU films upon UV/vis/NIR irradiation. Reprinted with permission.<sup>71</sup> Copyright 2019, Elsevier.





Scheme 3 The reaction scheme of the preparation of BHPU/TABA.

networks while breaking the intramolecular H-bonding in the PU network. In terms of light-responsive properties, the stretched BHPU/TABA film was curled under UV irradiation ( $\lambda = 365$  nm) and the *cis*-TABA/BHPU film remained stable under visible light irradiation ( $\lambda = 460$  nm). After UV exposure, the *cis*-TABA was fixed at lower temperature due to the vitrification of polymer chains and insufficient visible light, under which the *cis*-isomer could not overcome the steric hindrance.<sup>11,74</sup> However, the curled BHPU/TABA film was able to recover to the original shape by reheating to 80 °C (Fig. 8). As compared to the normal thermal-induced shape memory effect, the light-responsive shape memory does not require a certain temperature field and avoided the uncontrollable continuous heating during the application. This has shown the exceptional properties of the light-responsive BHPU/TABA complexes.

Chen *et al.* synthesized a dual light- and thermo-responsive SMPU by reacting polycaprolactone (PCL,  $M_n = 4000$  g mol<sup>-1</sup>) and diphenylmethane diisocyanate (MDI), followed by the reaction with 1,4-butanediol.<sup>73</sup> 4-(4-Oxyalkyl chain carbonyl) azodibenzoic acid (Azo11) was incorporated as a filler in the SMPU matrix by casting the SMPU and Azo11 in DMF solution onto a Teflon plate and left to dry at 80 °C. Azo11 (Scheme 4) was reported to enhance the crystallization capacity of the soft segment of SMPU and resulted in the curled Azo11-SMPU film that did not recover to the initial shape but fixed temporarily

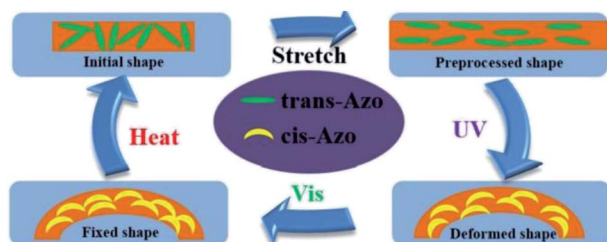
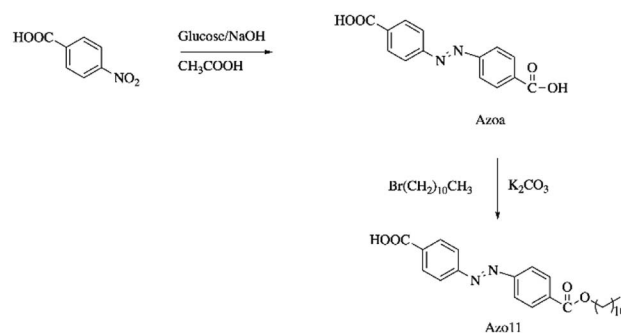


Fig. 8 Schematic illustration of the mechanism of photo-thermal staged-responsive shape memory properties in the molecular structure. Reprinted with permission.<sup>11</sup> Copyright 2019, Elsevier.

under visible light irradiation. The recovery of the SMPU was aided by heat. This unique characteristic is known as staging-responsive shape memory properties.<sup>74</sup> The Azo11-SMPU film first underwent UV light-triggered deformation, followed by fixation under visible light irradiation (that remained in a deformed shape), and thirdly, thermal-induced recovery into its original shape. These three stages are independently responsive to external UV, visible light, and heat stimuli. Upon exposure to UV light (365 nm), the Azo11 moieties isomerized from the *trans*-isomers to the *cis*-isomers, demonstrating the shrinkage of the azo11-PSMPU chain specifically on the film surface (film curling). The curling of the film was maintained for an extended time (>90 min) even though the film was irradiated by visible light (source and wavelength: not reported) due to the weak forces arising from the photoisomerization triggered by visible light, which was insufficient to destroy the intermolecular forces formed. The curled shape was able to recover to its original shape upon heating at 80 °C due to the crystal melting phase transition occurring at a higher temperature; thus, the increased energy aided the photoisomerization. The azo11-PSMPU has good potential applications in smart electronics, smart sensors, smart optical devices, and robotic fingers.

Yang *et al.* synthesized a dual light- and thermo-responsive staging SMPU by reacting HDI, PCL-4000, and Azoa, followed by the addition of glycerol as the crosslinker.<sup>12</sup> Scanning electron microscopy (SEM), atomic force microscopy (AFM), wide-angle X-ray diffraction (WAZRD), differential scanning calorimetry (DSC), and thermogravimetric (TG) results demonstrated that Azoa-SMPU formed microphase separation structures containing semi-crystallized PCL soft phase and an Azoa amorphous hard phase that could influence the crystallinity of the PCL soft phases. Upon UV irradiation, the stretched Azoa-SMPU film underwent deformation (bending) due to the isomerization of *trans*-Azoa to *cis*-Azoa. The deformation of Azoa-SMPU was reported to be due to the decreased distance between the PU chains in the *cis*-isomer form, which increased the hydrogen bonding of C=O and N=H. After UV exposure, the *cis*-Azoa isomers were fixed by strong intermolecular forces and the PCL crystalline soft phase; therefore, no recovery occurred under visible light. The author reported that the increased temperature caused the melting of the PCL soft



Scheme 4 The synthesis route of Azo11.



segments, thus destroying the hydrogen bonding of the hard segments and weakening the intermolecular forces of the polymer chains. Therefore, the deformation of shape was recovered at above 50 °C. With similar results of staging responsive SMPU, Ban *et al.* also investigated the same light-responsive group Azo but the final SMPU was recovered at 80 °C.<sup>74</sup>

**2.1.4. Light- and pH-responsive polyurethane containing azobenzene.** Mao *et al.* reported on the production of a dual light- and pH-responsive waterborne PU containing the Azo polymer by reacting IPDI and PCDL ( $M_w = 500 \text{ g mol}^{-1}$ ), followed by reacting with the synthesized *N,N*-dihydroxyethyl azobenzene<sup>6,93,94</sup> as a light chromophore.<sup>6</sup> The AZO-based PU exhibited reversible photoisomeric and acidichromic (responding to acid condition) properties. The AZO-chromophore with amino substituent in the *para*-position demonstrated acid chromic behavior, whereby the structure of the PU transfers from the diazo unit into the hydrazone form on reducing the pH from 6 to 1, which corresponds to a significant color change from yellow to pink (Fig. 9). The transformation of the azobenzene with tertiary amine group into hydrazone occurs under acidic environment, which resulted from the intramolecular proton transfer from the N-atom.<sup>6,95</sup> The AZO-based PU was reported to respond fast to UV illumination ( $\lambda = 365 \text{ nm}$ ) as a result of *trans*-to-*cis* photoisomerization of

azobenzene in both dry and solution state with the color changing from yellow (*trans*) to orange (*cis*). The reversible dual-responsive AZO-PU polymeric dye was proposed in the application of the sensor to monitor the environmental changes.

Li *et al.* reported on a dual light- and pH-responsive cationic waterborne PU (CWPU) with the side chain aromatic azobenzene group (AZO-CWPU) by reacting IPDI, polyether polyol, *N*-methyl diethanolamine, and EDPD *via* step growth polymerization.<sup>75</sup> The author reported that the incorporation of azobenzene increased the dipole moment of WPU, resulting in decreased static water contact angles and increased surface free energy coating as compared to the ordinary WPU. Upon UV irradiation at 365 nm, the static water contact angle was reduced from 61° to 55° due to the photoisomerization of azobenzene from the *trans*- to *cis*-form. The AZO-CWPU dispersion showed color change from red to yellow on increasing the pH values, which indicated the responsiveness of AZO-CWPU toward the change in the pH values. The AZO-PU dye existed in two equilibrium forms, *i.e.*, the hydrazone form and the azoic form, in acidic environment due to the formation of two symmetry centers and protonated nitrogen.<sup>75,96</sup> When the environment is more acidic, the hydrogen ions are attached to the nitrogen atoms of AZO-moieties and the diethylaminoethyl groups in AZO-PU; hence, the molecules became protonated. Under a weak acidic environment, the equilibrium of the hydrazone form and the azoic form was reached, and the mixture displayed an orange color. AZO-CWPU was also reported to be thermally more stable due to the good conjugation of the AZO moieties. The dual responsive AZO-CWPU was proposed to be potentially applied in optics and bioengineering areas.

**2.1.5. Light- and reductant-responsive polyurethane containing azobenzene.** Li *et al.* reported a dual light- and reductant-responsive AZO-PU hydrogel by reacting HDI and PEG-10000, followed by grafting with AZO, cyclodextrin (CD), and synthesized disulfide containing DSO.<sup>18</sup> The supramolecule possessed light-responsive properties due to the assembly of AZO and CD, whereas reductant responsiveness was contributed by the disulfide bond to provide environment responsiveness to the high elasticity of the hydrogel. The reduction in the swelling properties and the viscosity of the hydrogel were observed due to UV irradiation by the isomerization of the *trans*-AZO group to the *cis*-AZO group, which resulted in the exclusion of the hydrophobic AZO group from the CD cavity (Scheme 5a). UV irradiation reduced the water absorption properties of the AZO-PU hydrogel and visible light irradiation led to the recovery of the swelling properties. This was due to the UV irradiation transforming the *trans*- into the *cis*-AZO group, which is known to be more hydrophobic; thus, water was discharged from the hydrogel. The reductant, on the other hand, improved the swelling properties of the hydrogel due to the reductant cleaving the disulfide bond at the crosslinking points (Scheme 5b), which resulted in a decrease in the crosslinking density and loosened the hydrogel to accommodate more water. Coumarin-102 was used as a hydrophobic model drug in this work. It was reported that short UV irradiation duration improved drug loading into the AZO-PU hydrogel due to *trans*-AZO being

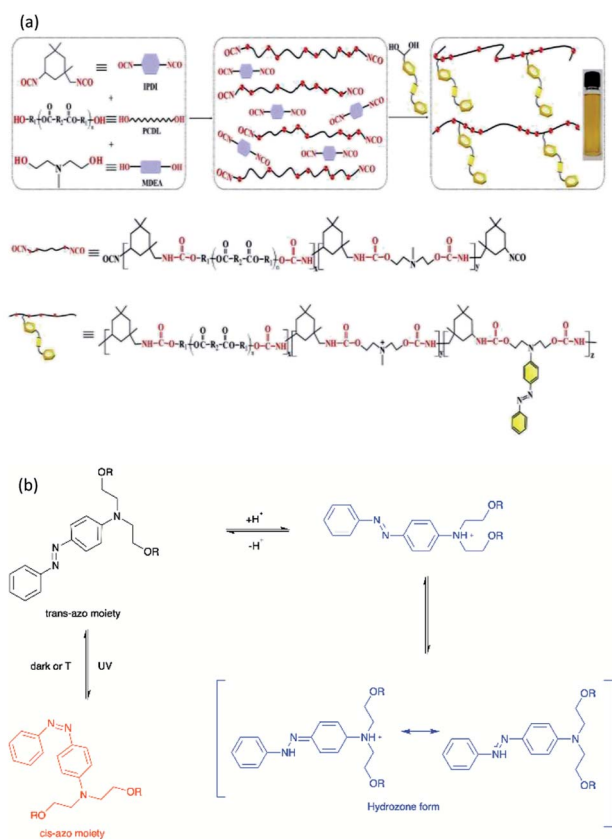
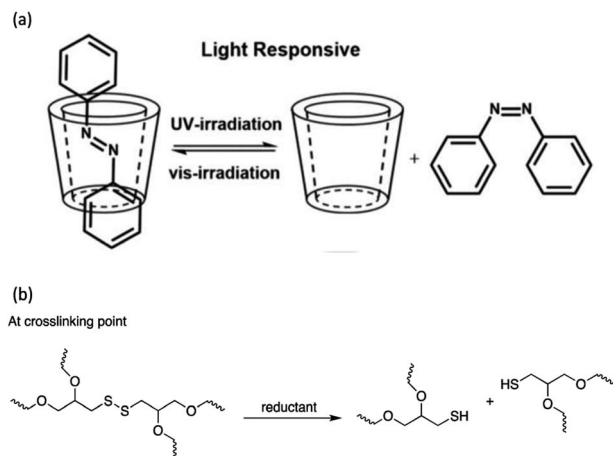


Fig. 9 (a) Synthesis route of the AZO-PU polymeric dye. Reprinted with permission.<sup>6</sup> Copyright 2018, Elsevier and (b) reaction scheme of the AZO moiety under UV light irradiation and acid condition.





Scheme 5 (a) Host-guest interaction of AZO. Reprinted with permission from L. Peng, S. Liu, A. Feng and J. Yuan, *Mol. Pharm.*, 2017, 14, 2475–2486.<sup>151</sup> Copyright 2017, American Chemical Society and CD under light irradiation and (b) the reductant breaks the disulfide bond and the crosslinkers are dissociated.

isomerized to *cis*-AZO (hydrophobic form), thus enabling the hydrophobic coumarin-102 to be loaded into the irradiated AZO-PU hydrogel. The AZO-PU hydrogel also reported the low cytotoxicity and was a prospective drug carrier.

## 2.2. Spiropyran-based polyurethane

Spiropyran (SP) is one of the unique organic chemical groups that contains dynamic covalent bond, in which the ring will be opened in response to UV and be converted to the colored merocyanine (MC) form.<sup>97</sup> The MC form reverts to stable SP under visible light or in dark situation (Fig. 2b). Different SP-based PU (SP-PU) have been reported for their UV activation and/or ultrasonic sensitive properties. SP is commonly involved in the preparation of optical devices,<sup>98</sup> biological imaging,<sup>99</sup> and chemical sensors.<sup>100,101</sup>

Zhang *et al.* presented an ionic WPU with dual light- and force-responsiveness.<sup>7</sup> Ionic WPU was synthesized by reacting IPDI and polytetramethylene glycol as well as the synthesized di-hydroxyl spiropyran (SP)<sup>7,102,103</sup> as the chain extender to produce an SP-WPU prepolymer, followed by reacting the SP-WPU prepolymer with dimethylolpropionic acid (DMPA) as the ionized segment and triethylamine (TEA) as the neutralizer. The ionic SP-WPU produced exhibited light-sensitive properties in both the emulsion and polymer film. The yellowish emulsion was turned to purple instantly upon exposure to UV light ( $\lambda = 365$  nm), which indicated the ring opening of SP (yellow) to form MC (purple) in the PU chain. The recovery process of the MC to the thermodynamically more stable SP form was induced by visible light or placing the WPU in dark. The author reported that the SP-WPU film had higher UV activation rate than the SP-WPU emulsion, which was due to the equilibrium reaction between SP and MC. As for the recovery rate, it was reported that the MC in the WPU emulsion form had a higher recovery rate than the WPU film because the light-sensitive molecule in the emulsion state could move more freely, thus taking lesser time for molecular conversion to a thermodynamically stable SP.

The author also investigated the mechanical responsiveness of SP-WPU by sonication and tensile test. The ultrasonication responsiveness properties of the SP-WPU dispersion relied on the water content due to the synergetic effect of the polarity of the mixed solvents. In terms of stretch responsiveness, the SP-WPU film showed blue color when stretching and changed to purple and pink when the film was unloaded. This secondary color change is due to the isomerization of the methane bridge in the activated MC.<sup>7,104</sup> SP-WPU was proposed for its potential application as a light sensitive coating material in sunglasses (Fig. 10).

## 2.3. Reversible light-induced dimerization reaction

The coumarin moieties and anthracene can perform photo-dimerization that were triggered by irradiating the PU under UV light (Fig. 2d). The UV-irradiated ( $\lambda = 365$  nm) coumarin dimers convert back to the original structure on irradiation at a wavelength of 254 nm.<sup>76</sup> The light-responsive coumarin can be crosslinked with other responsive functional groups (*e.g.*, pH-responsive groups) to produce PU material with greater targetability in drug delivery systems in order to improve the performance of the smart polymer with large variation of the physiological microenvironment.<sup>19</sup> This coumarin-based PU offers the possibility of using environment friendly materials with healing properties in smart coating applications.<sup>77,78</sup> On the other hand, the anthracene light-induced dimerization does not have a strict requirement of the wavelength of the UV-light source.<sup>44,79,105–107</sup> It has been reported that the anthracene groups undergo [4 + 4] cycloaddition reactions under UV light exposure ( $\lambda > 300$  nm) and the anthracene groups are regenerated by the scission of the dimers when they are irradiated with short wavelength UV light ( $\lambda < 300$  nm) or stimulated at a temperature above 120 °C.<sup>79</sup> The coumarin groups and anthracene groups were also reported to endow the PU with self-healing properties.<sup>77,79</sup>

The single and dual light- and pH-response of PU-containing coumarin as well as dual light- and thermo-responsive PU containing anthracene with light-induced dimerization are discussed in the following paragraphs.

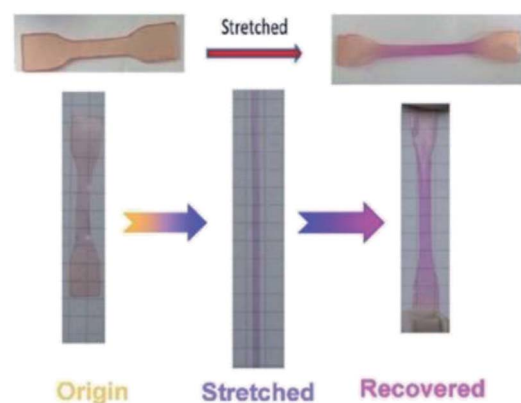


Fig. 10 The digital photos of stretch sensitive SP-WPU film. Reprinted under terms of the CC-BY license.<sup>7</sup> Copyright 2017, Royal Society of Chemistry.



**2.3.1. Coumarin-based polyurethane.** Aguirresarobe *et al.* produced a reversible light-responsive WPU by reacting IPDI and PPG-1000, followed by introducing the synthesized HMEC<sup>76,108</sup> in the chain ends of the PU prepolymer.<sup>76</sup> The particle size of WPU increased with HEMC, which indicates that the non-covalent interaction among the HEMC moieties influenced the particle size. The coumarin moieties incorporated in WPU underwent photodimerization, which was induced by the [2 + 2] cycloaddition reaction under UV light ( $\lambda = 365$  nm). This UV-induced reaction generated a cyclobutane ring by joining two coumarin molecules at the double bond sites (Scheme 6). When the coumarin-based PU was irradiated at 254 nm, the photocleavage reaction occurred and the dimers converted back to their original structures. It is noteworthy that the photocleavage reaction occurs faster than the [2 + 2] cycloaddition, especially when the radiation intensity is 254 nm. Later (2016), the same research group reported a similar synthesis method<sup>76</sup> but in addition incorporated the newly synthesized DHEMC as the chain extender in order to obtain the light-responsive PU with the addition of the self-healing properties.<sup>77</sup> The DHEMC found underwent the [2 + 2] cycloaddition reaction and caused crosslinking in the hard segment of the PU when it was irradiated with UV light ( $\lambda > 300$  nm). Besides, the cyclobutane ring in the coumarin dimers was cleaved and reverted to coumarin after exposure to UV light for 3 h at wavelength  $< 300$  nm. However, the crosslinked network prevented surface rearrangement and damage refilling, while the scratches were caused by the breaking of the PU chain and the enhancement of the chain mobility in the damaged areas. Nevertheless, when the films were exposed at 254 nm for one hour, the capability of refilling the scratches was partially recovered due to the decrosslinking of the PU network (Fig. 11). The selection of irradiation conditions, polymeric chain mobility on the fracture, as well as the capacity to generate the crosslinking polymer networks by coumarin linkages were proved to be the main factors affecting the self-healing process.

Salgado *et al.* reported the production of a light-responsive PU containing coumarin by reacting a coumarin diol-HDI prepolymer with PCL.<sup>78,109</sup> Silica nanoparticles (mSiNPs) were dispersed into the coumarin-based matrix. The mechanical and thermal properties of the PU were reported to be improved by the incorporation of the coumarin diol as the chain extender, while the coumarin offered its light-responsive properties to the final PU product. The coumarin moieties underwent reversible light-induced dimerization and photocleavage at 365 nm and 254 nm, respectively. The coumarin-based PU dispersed with mSiNP showed higher photodimerization behavior due to the good interaction between the mSiNPs and the hard segments of the PU matrix, as is evident by FTIR. The photodimerization yield was also higher than that of the photocleavage yield due to the equilibrium between the dimers and the cleaved coumarins after irradiation with UV light.<sup>110</sup> Photodimerization between the hard segment and mSiNPs were agglomerated, which are less likely to perform photocleavage. The drawback of the addition of coumarin diol into the PU matrix was the detrimental effect on the transparency of the PU matrices, causing

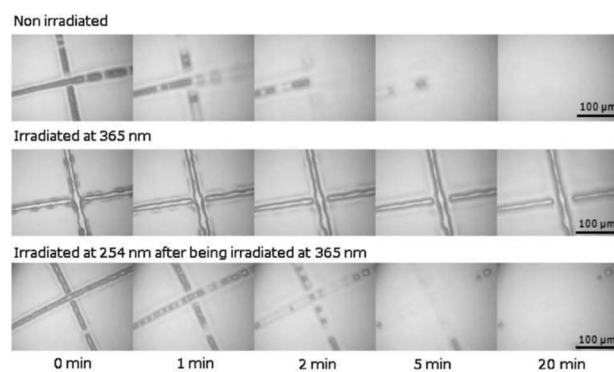
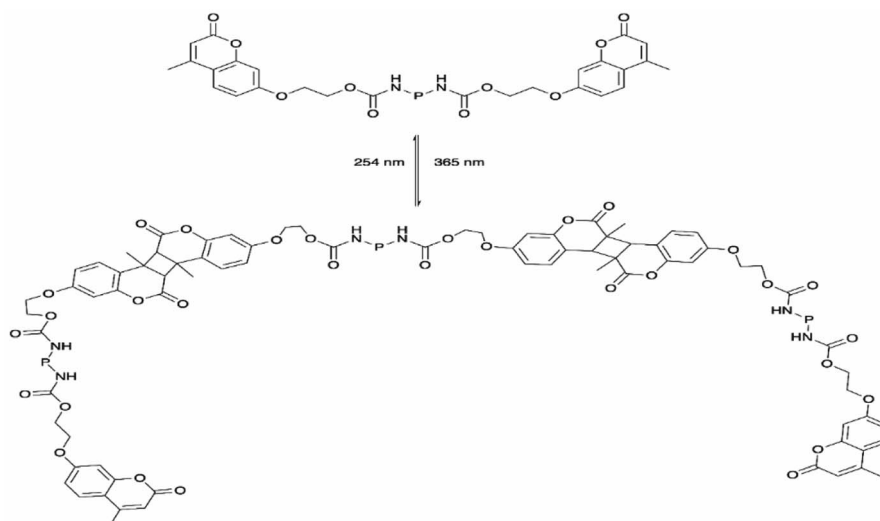


Fig. 11 Optical microscopy of coumarin-PU during the filling process. Reprinted with permission.<sup>77</sup> Copyright 2016, Elsevier.



Scheme 6 The reversible photoinduced [2 + 2] cycloaddition reaction of coumarin moieties.



a complete blocking effect in the region of the UV spectrum from 245 to 355 nm.

Long *et al.* utilized light-responsive coumarin derivatives and pH-responsive hydrazone groups in PU production for targeted cancer chemotherapy.<sup>19</sup> PU was produced by reacting L-lysine ethyl ester diisocyanate (LDI) and hydrophilic PEG-600 for a biocompatible micelle drug delivery PU system.<sup>19,111</sup> PU was further reacted with the newly synthesized coumarin derivative OMC<sup>19</sup> as the crosslinker *via* hydrazone bonding, followed by the introduction of folic acid (FA) into the PU network *via* amidation. The hydrophobic anticancer drug doxorubicin was encapsulated into the micelles by the dialysis method. The release profiles showed that the drug release rate at pH 5.8 was faster than at pH 7.4. The fast release of the drug was postulated to be related to the repulsion between the ionized amino groups at lower pH and led to looser nanoparticles, which caused the drugs to be more likely to diffuse out from the micelles. Upon UV irradiation at 365 nm, coumarin dimers were formed *via* the [2 + 2] cycloaddition formation of the cyclobutene ring<sup>19,112</sup> and the crosslinking of the micelles, as proved using UV-Vis spectroscopy. At wavelength 320 nm, the intensity of the peak of the OMC groups was reduced with the irradiation time, which showed the dimerization of the OMC groups and the crosslinking of the micelles. The crosslinking process reached the maximum yield with the increase in the irradiation time (~130 min), hence resulting in the rigidity of the polymer chain inside the micelle cores, which prevented the further dimerization of the OMC groups. The studies also reported that light-induced crosslinking did not exhibit toxicity and interrupt drug release in *in vitro* studies. The dual-responsive PU-containing coumarin micelles are potential drug carriers due to excellent stability in physiological environments after UV light-induced crosslinking and can release loaded drugs under low pH condition (*e.g.*, tumor cell) (Fig. 12). To date, dual light- and pH-responsive PU-containing coumarin that responded to visible or NIR light and meant for drug delivery have not been reported. The dual light- and pH-responsive PU-containing coumarin that responded to UV light also has limited applications in drug delivery due to UV light being unable to penetrate deeply into the body. Hence, research on smart PU with visible light- or NIR light-responsive

and pH-responsive is worth exploring for the emerging chemophototherapy for cancer treatment.

**2.3.2. Anthracene-based polyurethane with dual responsiveness: dual light- and thermo-responsiveness.** It has been reported that anthryl groups undergo reversible dimerization as [4 + 4] cycloaddition reactions under UV light irradiation with wavelength more than 300 nm. Alternatively, the anthracene (An) groups are reproduced by the scission of dimers either on irradiation with shorter UV wavelength ( $\lambda < 300$  nm) or heating above 120 °C.<sup>105–107,113</sup> [4 + 4] cycloaddition is a reaction, in which two unsaturated molecules were connected *via* four atoms from each molecule and formed a 8-membered ring with two new carbon-carbon bonds.

From the study conducted by Fang *et al.*, a novel dual light- and thermo-responsive PU film was produced by reacting IPDI and PPG-2000, followed by incorporating the anthracene diol derivative BHPAE, which endowed the PU films with dual responsiveness as well as self-healing properties.<sup>79</sup> The pendent anthracene groups underwent reversible [4 + 4] cycloaddition and formed a crosslinked structure when exposed to UV light ( $\lambda > 300$  nm) and reverted back when stimulated at a temperature above 130 °C. When the [4 + 4] cycloaddition reaction occurred, the carbon positions 9 and 10 of anthracene were dimerized as a result of the cleavage of the conjugated  $\pi$ - $\pi$  system of the anthracene groups. The rate of dimerization was fast, which reached the equilibrium state after 10 min of UV irradiation. The dimerization rate was reported to decrease when the number of photodimerization cycles increased due to the amount of restored anthracene groups that decreased with increasing cycles. The light-induced crosslinked structure reduced the mobility of the BHPAE-PU chains. The increased BHPAE contents also resulted in the rising of  $T_g$ . This means that the presence of anthracene increased the crosslinking density and further enhanced the thermal stability. The dual responsiveness reversible bonds located in the PU chain between the crosslinking points provided the BHPAE-PU with excellent self-healing ability. The mechanism of the healing process is as illustrated in Fig. 13. At the crack area, a majority of the dimers reverted back to anthracene monomers due to physical damage. The subsequent heating process guaranteed that the remaining dimers around the injured areas were cleaved and reverted to anthracene monomers. Meanwhile, the reduced crosslinking density permits the mobility of the PU chains at elevated temperature, which contributed to the

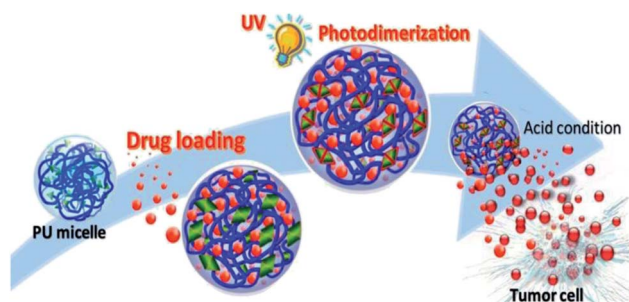


Fig. 12 Illustration of the core crosslinked polyurethane micelles for the intracellular release of anticancer drugs triggered by the acidic microenvironment inside the tumor cell. Adaptation under terms of the CC-BY license.<sup>152</sup> Copyright 2020, International Journal of Molecular Sciences.

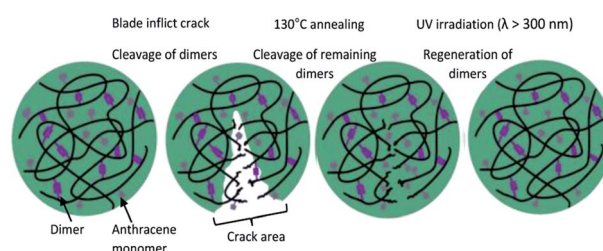


Fig. 13 The schematic illustration of the self-healing process of the PUAN films.

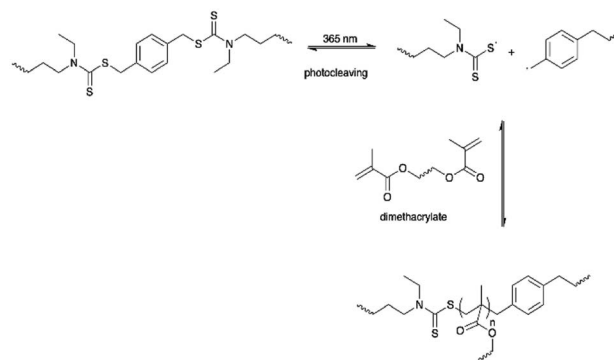


healing of cracks. The healing process completed after the dimers were regenerated under UV light illumination ( $\lambda > 300$  nm).

#### 2.4. Irreversible light-induced photocleavage reaction

The irreversible photocleavage reaction normally occurs in *o*-nitrobenzyl (*o*-NB)-incorporated polymers. The *o*-NB photocleavage groups can be located in the side chain, main chain, or as a cross-linker of copolymers.<sup>20</sup> After UV irradiation, the by-product of *o*-NB such as *o*-nitrosobenzaldehyde could act as an internal filter and hence reduced the *o*-NB cleavage efficiency.<sup>114</sup> However, the by-product could possibly react with amine to form an imine compound, which would cause problems to the nearby proteins (Scheme 7).<sup>115</sup>

A light-responsive PU system from a 2-amino-1,3-propanediol (serinol)-based monomer in which the amino group is protected by the *o*-NB group *via* a carbamate linker was developed by Sun and *et al.*<sup>20</sup> Upon UV light exposure, the *o*-NB groups underwent irreversible photocleavage reaction to release the functional amine groups, which further induced the partial degradation of the PU backbone *via* intramolecular cyclization (Fig. 14a). The author proposed that the degradation mechanism indicated that the addition of the base would speed up the degradation rate because the deprotonated amino groups are more nucleophilic. The light-responsive PU was formulated into nanoparticles, which was employed as the drug carrier for the encapsulation of the hydrophobic model drug Nile Red. On irradiation with UV light (320–480 nm), the light-responsive PU nanoparticles possessed a structural change, which resulted in the burst release of the hydrophobic Nile Red payload in the aqueous environment (pH 7.0) and reached maximum release within 20 seconds of UV light irradiation. Nevertheless, a NIR-



Scheme 8 The LBCL was photocleaved under 365 nm and further initiated light-induced methacrylate polymerization.

responsive moiety can be used for developing polymeric materials instead of UV-responsive moieties to obtain deeper tissue penetration.<sup>116</sup>

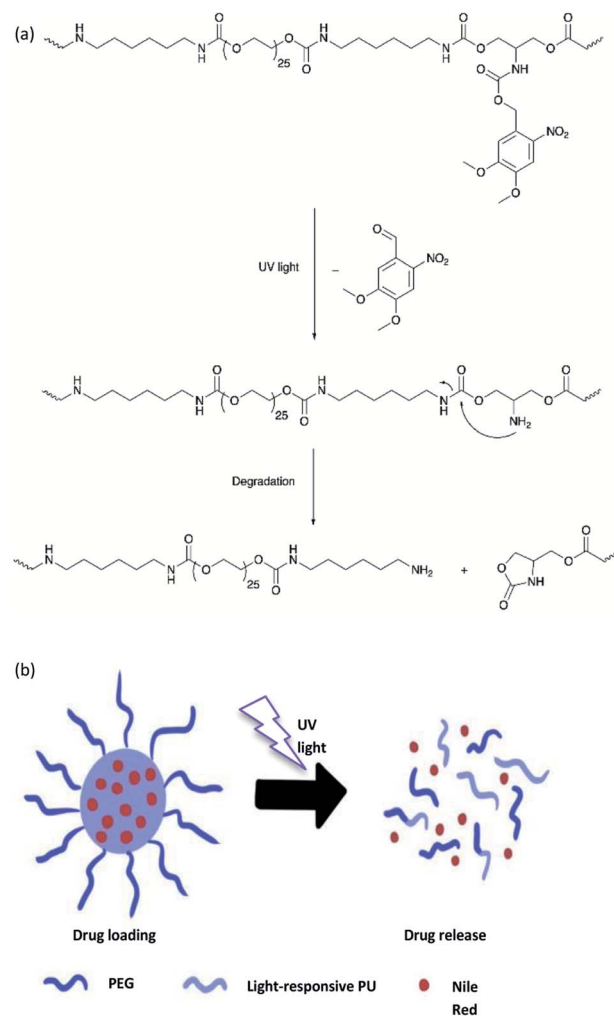


Fig. 14 (a) Reaction scheme of the photocleavage of *o*-NB and (b) schematic illustration of the formation and structural change of the light-responsive PU nanoparticles loaded with Nile Red as the model drug.

Scheme 7 (a) The photocleavage reaction of *o*-nitrobenzyl and (b) the reaction of *o*-nitrosobenzaldehyde and primary amine.



## 2.5. Light-induced crosslinking reaction

Light-induced crosslinking reaction is known as photopolymerization, such as the UV curing of multifunctional monomers to transform a liquid resin into a solid polymer almost instantly and selectively at the illuminated areas.<sup>117</sup> UV light curable materials mainly include oligomers, diluents/monomers, and a photoinitiator. The photoinitiator is an important reactant for the preparation of high-performance photopolymers. Photoinitiator can be used in free radical, cationic, and anionic polymerization and also helps to increase the photosensitivity in UV-curable PU. In the following section, the PUs will be crosslinked with acrylate or inorganic oligomers and further reinforced the physical properties of PU under the exposure of UV light<sup>80</sup> or visible light.<sup>118</sup>

**2.5.1. Acrylate-based polyurethane.** Bioprinting is a technology to directly print cells and biomaterials together for the construction of complex 3D functional living tissues.<sup>119</sup> Poor mechanical stability is one of the major concerns for 3D bioprinting materials because the structure printed from the polymer tends to collapse.

Hsiao *et al.* reported dual light- and thermo-responsive PU dispersions synthesized from PCL diol, oligodiol, and IPDI *via* the waterborne process.<sup>80</sup> 2-hydroxyethyl methacrylate (HEMA) groups were introduced at the end of the thermo-sensitive PU main chains as single hydroxyl acrylate to generate vinyl-terminated PU, where the acrylic functionality served as the UV-responsive curing site.<sup>80,119</sup> Photoinitiator 2,2'-azobis[2-methyl-N-(2-hydroxyethyl)propionamide] (VA-086) was incorporated to increase the cell viability<sup>80,120–122</sup> and initiate the light-induced crosslinking process. The UV light source ( $\lambda = 365$  nm) transmitted through the PU dispersion to excite the photoinitiator and initiate the UV-curing process. The PU nanoparticles (NP) showed light responsiveness, which gave rise to an increase in the molecular weight, particle size, and crosslinked network after UV irradiation. Furthermore, the cured PU NP became more rod-shaped and formed a compact structure after further heating. The UV-cured PU dispersion underwent a thermal-induced sol-gel transition at 37 °C and was able to recover the solid-like structure to obtain a stable construct. The UV-curable crosslinking network may limit the mobility of the polymer chain and reduce the free volume in a PU NP by decreasing the degree of swelling of the cured NP after further heating. Therefore, a shorter distance among the cured PU NPs may stimulate the formation of hydrogen bonding and undergo phase transition at higher temperatures, therefore enhancing the mechanical properties of the PU. There is no report on NIR light-induced crosslinking in PU.

Urethane oligomers are commonly used for high performance coating materials. In addition, PU is known for excellent weathering and chemical resistance of the coating and is usually used in a wide range of UV-curable coating materials.<sup>81,123,124</sup> Using different forms and concentrations of the reactive diluents, the adhesion, mechanical, and physical properties of the PU are possibly modified without altering the composition of the PU coating system. Zvonkina *et al.* reported on a UV-curable PU coating from the aliphatic difunctional urethane oligomer, functional acrylic reactive diluent, and

a mixture of photoinitiators, *i.e.*, Irgacure 184 and Irgacure 819.<sup>81</sup> The photopolymerization mechanism was employed in the film form of PU. The polymerization process was examined by measuring the heat flow under UV light irradiation (light source: Omnicure Series 2000 device, 160 W, wavelength: not reported) and was assessed by exothermic enthalpy during the photopolymerization process. The improvement of the PU coating adhesion while enhancing the coating flexibility in response to UV light was reported due to the crosslinking process during photopolymerization. The physical properties of the UV-curable coating can be modified according to the desired requirements by selecting the composition of the monomers.

Hu *et al.* reported the synthesis of a biobased cardanyl acrylate (CA) as a reactive diluent in an UV-curable castor oil-based polyurethane-acrylate (COPUA) by reacting cardanol and acryloyl chloride,<sup>9,125</sup> followed by the incorporation of Darocur1173 as the photoinitiator.<sup>9</sup> The modified PUA showed an improvement in the volumetric shrinkage and biobased carbon contents as compared to petroleum-based PU. Volumetric shrinkage is one of the major challenges for UV-curable acrylic, which may deform the final cured materials and affect the molding efficiency.<sup>9,126</sup> By incorporating CA, the hydrophobicity was increased due to the long hydrophobic alkyl chains scattered into the castor oil-based PUA matrix and prevented the penetration of water molecules.<sup>9,127</sup> The improvement in the physical properties such as hardness, adhesion, and thermal stability of PUA were related to the flexible long C15 alkyl chains and rigid benzene ring from cardanol. Nevertheless, the castor oil-based PUA coating system was rapidly cured (40 seconds) upon UV light irradiation. Higher CA content resulted in higher carbon-carbon double bonds conversion into single bonds (–C–C–). The higher CA content caused lower viscosity and thus increased the binding opportunities between the radicals and enhanced the carbon-carbon double bond conversion.<sup>9,128,129</sup>

Wang *et al.* reported a series of environment-friendly UV-curable PU coatings synthesized using acrylate polyester (APE) as oligomers with different non-isocyanate urethane dimethacrylate as reactive diluents.<sup>82</sup> The reactive diluents were 1-(methacryloyloxy)propan-2-yl 3-(methacryloyloxy)propylcarbamate (POAPD), 2-(methacryloyloxy)ethyl 3-(methacryloyloxy)propylcarbamate (POAED), and 2-(methacryloyloxy)ethyl 2-(methacryloyloxy)ethylcarbamate (EOAED). Darocur 4265 was selected as the free radical photoinitiator. The introduction of urethane dimethacrylate could decrease the viscosity of the APE oligomer for ease of processing. Upon UVB irradiation at a wavelength of 257 nm, the photoinitiator was activated and initiated photopolymerization to crosslink the PU network. The toughness of the PU coating was enhanced due to the formation of hydrogen bonds from N–H and C=O groups in the urethane groups as a result of the crosslinking in the PU matrix, which was triggered by UVB irradiation. Besides, the  $T_g$  of PU increased with the increase in the crosslinking density of the PU system, which contributed to better thermal stability of the UV-cured PU.<sup>82,130</sup>

**2.5.2. Inorganic-based polyurethane.** Mendes-Felipe *et al.* reported a combination of solvent free UV-curable PU acrylate/multi-walled carbon nanotube (PUA/MWCNT) for piezoresistive sensing by reacting commercially available polyurethane acrylate



photoresin SPOT-E™ and MWCNT (NC7000™) as carbon-based piezoresistive material.<sup>10</sup> The incorporation of MWCNT into the PUA polymer matrix affects the UV curing process at a wavelength of 395 nm due to its light absorption and reduced the  $T_g$  of PU, which also further reduced both acrylic C=C double bond conversion and photopolymerization rate due to the competition of light adsorption with the photoinitiator<sup>10,131</sup> and high conversion at the immobilization of the polymer chains caused by the UV curing reaction.<sup>10,132</sup> The decrease in the  $T_g$  was due to the nanofillers' plasticizing effect that led to a larger free volume within the polymer with increasing MWCNT content.<sup>10,133</sup> Nevertheless, the uniform dispersion of the MWCNT enhanced the electrical conductivity due to the low electrical percolation thresholds,<sup>10,134</sup> while it still maintained the mechanical properties of the PUA matrix. MWCNT showed increased mechanical strength than the PUA matrix. PUA/MWCNT was also reported for good wettability due to the fillers and its prospect in sensor applications.<sup>10,135–137</sup>

Huang *et al.* reported on a UV-curable PU system consisting of the UV-sensitive phosphazene acrylate (NPHE) monomer, PUA oligomer, and a photoemitter.<sup>8</sup> The PU system was first prepared by reacting PPG-2000 and IPDI to obtain NCO-terminated PU prepolymer, followed by reaction with HEMA to form the PUA polymer. The UV-sensitive phosphazene monomer was derived from the HEMA substitution reaction to hexachlorocyclotriphosphazene (NPCl<sub>2</sub>)<sub>3</sub> and incorporated into the PUA polymer. The thermal stability of NPHE-PU was slightly increased due to crosslinking between the PU polymer main chains and the NPHE monomer stimulated by the UV irradiation. In addition, the final UV-curable NPHE-PU film also reported improved thermal, physical, and mechanical properties. On the other hand, NPHE-PU also demonstrated the flame-inhibition properties because the presence of phosphorus and nitrogen compositions of NPHE producing non-flammable nitrogen oxides and phosphorus oxides during combustion prevented air supply on the material surface and thus inhibited combustion at elevated temperature. The multifunctional UV-sensitive NPHE was proposed to be used as a flame retardant, diluent, and crosslinker in the UV-curable PU coating system.

A polyester PU particle was prepared by the reaction of PEG with PU particles, followed by the addition of nanosized negative ion powder to obtain the PU negative ion (PU/NI) film *via* a non-solvent-induced phase separation method.<sup>83</sup> The negative ion powder (NI) is a kind of complex inorganic material used to accelerate the adsorption of the silver precursor due to its strong electronegativity.<sup>83,138</sup> Subsequently, the Ag<sub>3</sub>PO<sub>4</sub>@AgBr nanoparticles, Ag<sub>3</sub>PO<sub>4</sub> and AgBr were loaded *in situ* onto the PU/NI film by the impregnation–precipitation-ion exchange method.<sup>83,139</sup> In order to compare the results from individual photocatalysts and combine them, the authors prepared three films for comparison, *i.e.*, Ag<sub>3</sub>PO<sub>4</sub>-PU/NI, AgBr-PU/NI, and Ag<sub>3</sub>PO<sub>4</sub>@AgBr-PU/NI. The recyclability and photocatalytic activity of the films were evaluated by the degradation of methyl orange in the recycling process under visible light exposure ( $\lambda > 420$  nm). At the beginning, the partial transformation of Ag<sup>+</sup> ions into metallic Ag NPs occurred *via* the reduction effect of photogenerated electrons.<sup>83,140–142</sup> Hence, strong surface plasmon resonance (SPR) effect enhanced

the photocatalytic activity of the films. Furthermore, the energy band structure of Ag<sub>3</sub>PO<sub>4</sub> and AgBr facilitated the electron–hole separation. Upon visible light exposure, Ag<sub>3</sub>PO<sub>4</sub> and AgBr within the PU/NI films were excited to photogenerate electrons and holes in their conduction and valence bands. The holes that were generated by the surface plasmons due to the resonance (SPR) effect on the Ag NP could directly oxidize the organic dye. The introduction of AgBr into the Ag<sub>3</sub>PO<sub>4</sub>-PU/NI film was also reported to synergistically enhance the photocatalytic activity of the film in degrading organic pollutants due to the reduced recombination rate of the electron–hole pairs, resulting from the heterojunction between AgBr and Ag<sub>3</sub>PO<sub>4</sub> that formed on the Ag<sub>3</sub>PO<sub>4</sub>@AgBr-PU/NI film.<sup>83,143</sup> The Ag<sup>+</sup> ions from the Ag<sub>3</sub>PO<sub>4</sub>-PU/NI, AgBr-PU/NI, and Ag<sub>3</sub>PO<sub>4</sub>@AgBr-PU/NI films damaged the bacterial protein and intracellular organelles.<sup>83,144,145</sup>

## 2.6. Fluorescent dye

Rhodamine (Rh) is a widely used fluorescent chromophore with excellent optical properties of good stability and quantum efficiency. The derivatives of rhodamine have been used widely in industrial coloration, fluorometric probes, and fluorescent labelling of biomolecules for a new photochromic system.<sup>146,147</sup> Rhodamine B can be incorporated in SMPU to increase the sensitivity of SMPU toward UV light with reversible photochromic behavior.<sup>84</sup>

Cai *et al.* reported that a dual light- and thermo-responsive SMPU composite was prepared from a commercial available poly(ester urethane) (Desmopan DP 2795A SMP) as a multifunctional PU composite that was composed of MDI and 1,4-butanediol as a chain extender, whereas soft segments were based on poly(1,4-butylene adipate),<sup>1,84</sup> followed by the reaction with functionalized microcrystal cellulose (20  $\mu$ m) as a dual functional modifier that acts as a crosslinker and a reinforcement agent.<sup>84</sup> Meanwhile, RhB was incorporated as a toughening modifier to enhance the UV sensitivity and generated a light-responsive SMPU. The RhB-based PU films showed thermally induced shape memory effect, which can be addressed by the H-bonding and chemical crosslinking. The deformed PU film was fixed at 0 °C and recovered to its initial shape after reheating to 60 °C. The flexibly chemically crosslinked RhB and hard segment of PU contributed to the toughness and shape memory effect. RhB also demonstrated reversible photochromic behavior as evident by the clear PU solution that turned pale pink under UV light exposure at 365 nm wavelength, while the PU solution was gradually changed back to a clear solution after heating at 80 °C for 30 min. This is because the RhB surface spiroamide groups were switched reversibly from non-fluorescent (ring-closed structure) to fluorescent (ring-opened structure) in response to UV illumination or heating.<sup>84,148</sup>

## 2.7. Other photochromic groups

Gordon *et al.* developed a light-induced PU with simultaneous healing and strengthening properties by reacting HDI with triethanolamine.<sup>85</sup> The authors introduced a photoactive dithiocarbamate iniferter unit containing carbon-sulfur (C–S) bonds as a labile bond crosslinker (LBCL) and ethylene glycol



dimethacrylate in the PU network. The C–S bonds underwent photocleaving under UV light ( $\lambda = 365$  nm) and generated a radical to initiate the first free radical polymerization on the dimethacrylate monomers. Thus, secondary polymerization occurred to give greater crosslinking density, which further enhanced the network modulus and strengthened the PU. LBCL differed from photoinitiators since the photoinitiators normally terminate after light irradiation but the radicals produced from dithiocarbamate iniferter in this PU system reversibly recombined and allowed radical generation within the PU network and be constantly induced using light.<sup>85,149,150</sup> The iniferter acted as a macroinitiator triggered by UV light and initiated free radical polymerization that increases the network modulus and at the same time aids in healing the PU materials after damage. The authors proposed the development of a formulation for other applications that may require secondary polymerization such as wrinkling and surface functionalization (Scheme 8).<sup>85,150</sup>

### 3. Conclusion and future aspects

In this review, different light-responsive groups are incorporated into the PU matrix to endow responsiveness toward light. These light-responsive PUs have been designed into biosensors, drug carriers, shape memory polymer for biomimetic robot, coating for optical device, and fabric. The light-responsive regions of the respective PUs have also been highlighted. For better understanding, schematic illustration and reaction scheme are also included to illustrate the chemical light-induced reactions. Light as a stimulus is particularly attractive due to its availability. However, the essential element of light-responsive polyurethane is a light-sensitive moiety and its requirement for a specific wavelength of light, which may limit its practical applications. At present, light-responsive PU is commonly developed for mechanical applications such as coating, shape memory polymers, or electronic sensors. Although PUs have been known for their biocompatibility, the use of light-responsive PU for medical, biomedical, and pharmaceutical applications remains largely unexplored. This is due to the toxicity, biocompatibility, and biodegradability of the light-responsive group and its photo-reaction products are still not fully understood. Moreover, the restriction of safety measurement in medical and biomedical applications is the current challenge for light-responsive polymers. Further investigation is also needed to explore the feature of light-responsive PU and broaden its application in different areas.

### Abbreviations

5CAZ	4-Cyano-4'-pentylxyazobenzene
EHAB	4'-Ethyloxy-4-(11-hydroxyundecyloxy)-azobenzene
PE	Polyester
AZO	Azobenzene
EVA	Poly(ethylene-co-vinyl acetate)

PEG	Polyethylene glycol
Azo11	4-(4-Oxyalkyl chain carbonyl)azodibenzoic acid
GO	Graphene oxide
PNIPAM	Poly( <i>N</i> -isopropylacrylamide)
Azoa	4,4-Azodibenzoic acid
HDI	Hexamethylene diisocyanate
PPG	Polypropylene glycol
BHPAE	3-( <i>N,N</i> -Bis(2-hydroxyethyl)amine)propionic acid-9-anthracenemethanol ester
HMEC	7-(Hydroxyethoxy)-4-methylcoumarin
PU	Polyurethane
BTAEAZO	4-Butoxy-4'-(trimethylaminoethoxy)azobenzene
IPDI	Isophorone diisocyanate
RhB	Rhodamine B
BWPU	Dye-bonded blocked waterborne polyurethane
LDI	L-Lysine ethyl ester diisocyanate
SCLCPU (AZO)-N	Pentaerythritol
CNT	Carbon nanotube
MC	Merocyanine
SMPU	Shape memory polyurethane
DAB	4,4'-Diaminoazobenzene
MDI	Diphenylmethane diisocyanate
SP	Spiropyran
DHAB	Dihydroxyazobenzene
<i>o</i> -NB	<i>o</i> -Nitrobenzyl
TABA	4-Octyldecyloxybenzoic acid
DHEMC	7-Bis(2-hydroxyethoxy)-4-methylcoumarin
TDI	Toluenediisocyanate
DSO	3,3'-Disulfanediyldipropene-1,2-diol
OMC	4-Methyl-7-((4-oxopentyl)oxy)-2 <i>H</i> -chromen-2-one
$T_g$	Glass transition temperature
EDPD	2,20-(4-((4-Ethylphenyl)diazanyl)phenylazanediyldiethanol
PCDL	Polycarbonate diols
WPU	Waterborne polyurethane

### Author contributions

Ki Yan, Lam: investigation, methodology, visualization, writing – original draft & editing. Choy Sin, Lee: conceptualization, methodology, visualization, supervision, investigation, writing – review & editing. Mallikarjuna Rao, Pichika: supervision, methodology, writing – review & editing. Sit Foon, Cheng: supervision, methodology, writing – review. Rachel Yie Hang, Tan: investigation, methodology, writing – original draft.

### Conflicts of interest

There are no conflicts to declare.

### Acknowledgements

The authors would like to acknowledge the Fundamental Research Grant Scheme (FRGS) for financial support (Grant No. FRGS/1/2019/STG07/IMU/02/1)



## Notes and references

- 1 L. Peponi, M. P. Arrieta, A. Mujica-Garcia and D. López, *Modif. Polym. Prop.*, 2017, 131–154.
- 2 D. Wang, M. D. Green, K. Chen, C. Daengngam and Y. Kotsuchibashi, *Int. J. Polym. Sci.*, 2016, **2016**, 2–4.
- 3 C. Hazra, D. Kundu and A. Chatterjee, *Stimuli-responsive nanocomposites for drug delivery*, Elsevier Inc., 2018.
- 4 B. Jeong, S. W. Kim and Y. H. Bae, *Adv. Drug Delivery Rev.*, 2002, **54**, 37–51.
- 5 K. Petcharoen and A. Sirivat, *Curr. Appl. Phys.*, 2013, **13**, 1119–1127.
- 6 H. Mao, L. Lin, Z. Ma and C. Wang, *Sens. Actuators, B*, 2018, **266**, 195–203.
- 7 Q. Zhang, Y. Wang, C. Xing, Y. Cai, K. Xi and X. Jia, *RSC Adv.*, 2017, **7**, 12682–12689.
- 8 W. K. Huang, K. J. Chen, J. T. Yeh and K. N. Chen, *J. Appl. Polym. Sci.*, 2002, **85**, 1980–1991.
- 9 Y. Hu, Q. Shang, J. Tang, C. Wang, F. Zhang, P. Jia, G. Feng, Q. Wu, C. Liu, L. Hu, W. Lei and Y. Zhou, *Ind. Crops Prod.*, 2018, **117**, 295–302.
- 10 C. Mendes-Felipe, J. Oliveira, P. Costa, L. Ruiz-Rubio, A. Iregui, A. González, J. L. J. L. J. L. Vilas and S. Lanceros-Mendez, *Eur. Polym. J.*, 2019, **120**, 109226.
- 11 Y. Li, H. Zhuo, H. Chen and S. Chen, *Polymer*, 2019, **179**, 121671.
- 12 J. Yang, H. Wen, H. Zhuo, S. Chen and J. Ban, *Polymers*, 2017, **9**, 287.
- 13 N. Shelke, R. Nagarale and S. Kumbar, *Natural and Synthetic Biomedical Polymers*, 2014, pp. 123–144.
- 14 L. Zhou, Q. Liu, X. Lv, L. Gao, S. Fang and H. Yu, *J. Mater. Chem. C*, 2016, **4**, 9993–9997.
- 15 H. Xie, J. Shao, Y. Ma, J. Wang, H. Huang, N. Yang, H. Wang, C. Ruan, Y. Luo, Q.-Q. Wang, P. K. Chu and X.-F. Yu, *Biomaterials*, 2018, **164**, 11–21.
- 16 L. Yang, R. Tong, Z. Wang and H. Xia, *ChemPhysChem*, 2018, **19**, 2052–2057.
- 17 Q. Zheng, Z. Ma and S. Gong, *J. Mater. Chem. A*, 2016, **4**, 3324–3334.
- 18 J. Li, L. Ma, G. Chen, Z. Zhou and Q. Li, *J. Mater. Chem. B*, 2015, **3**, 8401–8409.
- 19 Y.-B. Long, W.-X. Gu, C. Pang, J. Ma and H. Gao, *J. Mater. Chem. B*, 2016, **4**, 1480–1488.
- 20 J. Sun, T. Rust and D. Kuckling, *Macromol. Rapid Commun.*, 2019, **40**, 5–9.
- 21 C. Yang, K. K. Chan, G. Xu, M. Yin, G. Lin, X. Wang, W. J. Lin, M. D. Birowosuto, S. Zeng, T. Ogi, K. Okuyama, F. A. Permatasari, F. Iskandar, C. K. Chen and K. T. Yong, *ACS Appl. Mater. Interfaces*, 2019, **11**, 2768–2781.
- 22 A. Bagheri, C. Boyer and M. Lim, *Macromol. Rapid Commun.*, 2019, **40**, 1–7.
- 23 J. H. Park, D. I. Kim, S. G. Hong, H. Seo, J. Kim, G. D. Moon and D. C. Hyun, *Pharmaceutics*, 2019, **11**, 528.
- 24 D. Park and J. C. Kim, *Int. J. Pharm.*, 2019, **554**, 420–428.
- 25 S. Machida, Y. Nakamura, A. Itaya and N. Ikeda, *Macromol. Chem. Phys.*, 2019, **1900240**, 1–7.
- 26 C. Zhao, J. Lu and X. X. Zhu, *ACS Appl. Polym. Mater.*, 2020, **2**, 256–262.
- 27 M. Wang, K. He, J. Li, T. Shen, Y. Li, Y. Xu, C. Yuan and L. Dai, *J. Biomater. Sci., Polym. Ed.*, 2020, **31**, 849–868.
- 28 J. Li, X. Li, H. Liu, T. Ren, L. Huang, Z. Deng, Y. Yang and S. Zhong, *Polym. Degrad. Stab.*, 2019, **168**, 108956.
- 29 J. Tian, B. Huang, C. Xiao and P. Vana, *Polym. Chem.*, 2019, **10**, 1610–1618.
- 30 M. Kang, A. N. Cha, S. A. Lee, S. K. Lee, S. Bae, D. Y. Jeon, J. M. Hong, S. Fabiano, M. Berggren and T. W. Kim, *Org. Electron.*, 2019, 105554.
- 31 H. Zhang, J. Zhou, G. G. Shan, G. F. Li, C. Y. Sun, D. X. Cui, X. L. Wang and Z. M. Su, *Chem. Commun.*, 2019, **55**, 12328–12331.
- 32 Y. Cozzens, D. M. Steeves, J. W. Soares and J. E. Whitten, *Macromolecules*, 2019, **52**, 2900–2910.
- 33 J. Anderski, L. Mahlert, J. Sun, W. Birnbaum, D. Mulac, S. Schreiber, F. Herrmann, D. Kuckling and K. Langer, *Int. J. Pharm.*, 2019, **557**, 182–191.
- 34 M. Lapshina, A. Ustyugov, V. Baulin, A. Terentiev, A. Tsvadze and N. Goldshleger, *J. Photochem. Photobiol., B*, 2020, **202**, 111722.
- 35 J. H. Choi, H. Seo, J. H. Park, J. H. Son, D. I. Kim, J. Kim, G. D. Moon and D. C. Hyun, *Colloids Surf., B*, 2019, **173**, 258–265.
- 36 C. Yin, X. Li, G. Wen, B. Yang, Y. Zhang, X. Chen, P. Zhao, S. Li, R. Li, L. Wang, C. S. Lee and L. Bian, *Biomaterials*, 2020, **232**, 119684.
- 37 Z. Wang, B. Guo, E. Middha, Z. Huang, Q. Hu, Z. Fu and B. Liu, *ACS Appl. Mater. Interfaces*, 2019, **11**, 11167–11176.
- 38 Z. Luo, L. Jiang, S. Yang, Z. Li, W. M. W. Soh, L. Zheng, X. J. Loh and Y. L. Wu, *Adv. Healthcare Mater.*, 2019, **8**, 1–13.
- 39 K. Poudel, R. K. Thapa, M. Gautam, W. Ou, Z. C. Soe, B. Gupta, H. B. Ruttala, H. N. Thuy, P. C. Dai, J. H. Jeong, S. K. Ku, H. G. Choi, C. S. Yong and J. O. Kim, *Nanomed. Nanotechnol. Biol. Med.*, 2019, **21**, 102042.
- 40 L. Li, Z. Yang, S. Zhu, L. He, W. Fan, W. Tang, J. Zou, Z. Shen, M. Zhang, L. Tang, Y. Dai, G. Niu, S. Hu and X. Chen, *Adv. Mater.*, 2019, **31**, 1–9.
- 41 Y. Xu, J. Chen, L. Tong, P. Su, Y. Liu, B. Gu, B. Bao and L. Wang, *J. Controlled Release*, 2019, **293**, 94–103.
- 42 J. Shin, J. Sung, M. Kang, X. Xie, B. Lee, K. M. Lee, T. J. White, C. Leal, N. R. Sottos, P. V. Braun and D. G. Cahill, *Proc. Natl. Acad. Sci. U. S. A.*, 2019, **116**, 5973–5978.
- 43 Y. Zhou, J. Tan, D. Chong, X. Wan and J. Zhang, *Adv. Funct. Mater.*, 2019, **29**, 1–8.
- 44 Y. Wu, Z. Hu, H. Huang and Y. Chen, *Polym. Chem.*, 2019, **10**, 1537–1543.
- 45 X. Di, Y. Kang, F. Li, R. Yao, Q. Chen, C. Hang, Y. Xu, Y. Wang, P. Sun and G. Wu, *Colloids Surf., B*, 2019, **177**, 149–159.
- 46 M. Evci, A. Tevlek, H. M. Aydin and T. Caykara, *Appl. Surf. Sci.*, 2020, **511**, 145572.
- 47 T. Sajini, R. Thomas and B. Mathew, *Polymer*, 2019, **173**, 127–140.



- 48 V. Marturano, V. Bizzarro, V. Ambrogi, A. Cutignano, G. Tommonaro, G. R. Abbamondi, M. Giamberini, B. Tytkowski, C. Carfagna and P. Cerruti, *Polymers*, 2019, **11**, 1–10.
- 49 T. J. Ahn, G. S. Seo and O. R. Lim, *IEEE Photonics Technol. Lett.*, 2019, **31**, 987–989.
- 50 T. Guan, Z. Du, X. Chang, D. Zhao, S. Yang, N. Sun and B. Ren, *Polymer*, 2019, **178**, 121552.
- 51 F. Jasinski, T. R. Guimarães, S. David, C. Suniary, T. Funston, Y. Takahashi, Y. Kondo and P. B. Zetterlund, *Macromol. Rapid Commun.*, 2019, **40**, 1900355.
- 52 R. D. Corder, J. C. Tilly, W. F. Ingram, S. Roh, R. J. Spontak and S. A. Khan, *ACS Appl. Polym. Mater.*, 2020, **2**, 394–403.
- 53 C. Yongli, C. Xiaolong, Z. Yating and Y. Jianquan, *J. Appl. Phys.*, 2019, **125**, 193102.
- 54 B. Sivaranjini, K. Mohana, S. Esakkimuthu, V. Ganesh and S. Umadevi, *Liq. Cryst.*, 2020, 1–12.
- 55 J. Wang, Q. Jiang, X. Hao, H. Yan, H. Peng, B. Xiong, Y. Liao and X. Xie, *RSC Adv.*, 2020, **10**, 3726–3733.
- 56 C. Wang, T. Hu, Y. Chen, Y. Xu and Q. Song, *ACS Appl. Mater. Interfaces*, 2019, **11**, 22332–22338.
- 57 H. Xie, L. Li, C. Y. Cheng, K. K. Yang and Y. Z. Wang, *Compos. Sci. Technol.*, 2019, **173**, 41–46.
- 58 D. Martella, S. Nocentini, F. Micheletti, D. S. Wiersma and C. Parmeggiani, *Soft Matter*, 2019, **15**, 1312–1318.
- 59 H. Yang, H. Wang, J. Feng, Y. Ye and W. Liu, *Macromol. Chem. Phys.*, 2019, **220**, 1–5.
- 60 J. Yu, K. Li, L. Li, L. Liu, Y. Zhou, Z. Zhang, M. Guo, N. Zhou and X. Zhu, *Polym. Chem.*, 2019, **10**, 2872–2880.
- 61 Y. Yuan, L. He, J. Li and H. Zhang, *Polym. Chem.*, 2019, **10**, 2706–2715.
- 62 J. Lee, J. M. Park and W. D. Jang, *Carbohydr. Polym.*, 2019, **221**, 48–54.
- 63 Q. Zhang, C. Tan, X. Zheng, P. Chen, M. Zhuo, T. Chen, Z. Xie, F. Wang, H. Liu, Y. Liu, X. Zhang, W. Lv and G. Liu, *Environ. Sci.: Nano*, 2019, **6**, 2577–2590.
- 64 A. C. Ferahian, D. K. Hohl, C. Weder and L. Montero de Espinosa, *Macromol. Mater. Eng.*, 2019, **304**, 1–10.
- 65 K. A. Bonetti, M. Murphy, R. L. Brainard, L. Zhong and J. T. Welch, *J. Polym. Sci.*, 2020, 1–5.
- 66 J. Lee, W. Lee, D. Kim, M. Kim and J. Kim, *Sci. Rep.*, 2019, **9**, 1–7.
- 67 H. Inoue, T. Hirai, H. Hanochi, K. Oyama, H. Mayama, Y. Nakamura and S. Fujii, *Macromolecules*, 2019, **52**, 708–717.
- 68 T. Fang, L. Cao, S. Chen, J. Fang, J. Zhou, L. Fang, C. Lu and Z. Xu, *Mater. Des.*, 2018, **144**, 129–139.
- 69 S. Li, Y. Tu, H. Bai, Y. Hibi, L. W. Wiesner, W. Pan, K. Wang, E. P. Giannelis and R. F. Shepherd, *Macromol. Rapid Commun.*, 2019, **40**, 1800815.
- 70 S. Chen, W. Zhang, C. Wang and S. Sun, *Green Chem.*, 2016, **18**, 3972–3980.
- 71 P. Zhang, B. Wu, S. Huang, F. Cai, G. Wang and H. Yu, *Polymer*, 2019, **178**, 121644.
- 72 Z.-B. Wen, D. Liu, X.-Y. Li, C.-H. Zhu, R.-F. Shao, R. Visvanathan, N. A. Clark, K.-K. Yang and Y.-Z. Wang, *ACS Appl. Mater. Interfaces*, 2017, **9**, 24947–24954.
- 73 S. Chen, J. Ban, L. Mu and H. Zhuo, *Polym. Chem.*, 2018, **9**, 576–583.
- 74 J. Ban, L. Mu, J. Yang, S. Chen and H. Zhuo, *J. Mater. Chem. A*, 2017, **5**, 14514–14518.
- 75 J. Li, X. Zhang, J. Gooch, W. Sun, H. Wang and K. Wang, *Polym. Bull.*, 2015, **72**, 881–895.
- 76 R. H. H. Aguirresarobe, L. Irusta, M. J. Fernández-Berridi, M. J. F.-B. L Irusta, L. Irusta and M. J. Fernández-Berridi, *J. Polym. Res.*, 2014, **21**, 505.
- 77 R. H. Aguirresarobe, L. Martin, N. Aramburu, L. Irusta and M. J. Fernandez-Berridi, *Prog. Org. Coat.*, 2016, **99**, 314–321.
- 78 C. Salgado, M. P. Arrieta, L. Peponi, D. López and M. Fernández-García, *Prog. Org. Coat.*, 2018, **123**, 63–74.
- 79 Y. Fang, X. Du, Z. Du, H. Wang and X. Cheng, *J. Mater. Chem. A*, 2017, **5**, 8010–8017.
- 80 S.-H. Hsiao and S.-H. Hsu, *ACS Appl. Mater. Interfaces*, 2018, **10**, 29273–29287.
- 81 I. J. Zvonkina and M. Hilt, *Prog. Org. Coat.*, 2015, **89**, 288–296.
- 82 X. Wang and M. D. Soucek, *Prog. Org. Coat.*, 2013, **76**, 1057–1067.
- 83 X. Wang, J. Jian, Z. Yuan, J. Zeng, L. Zhang, T. Wang and H. H. Zhou, *Eur. Polym. J.*, 2020, **125**, 109515.
- 84 C. Cai, Z. Wei, X. Wang, C. Mei, Y. Fu and W. H. Zhong, *J. Mater. Chem. A*, 2018, **6**, 17457–17472.
- 85 M. B. Gordon, J. M. French, N. J. Wagner and C. J. Kloxin, *Adv. Mater.*, 2015, **27**, 8007–8010.
- 86 K. Nagai and M. Katayama, *Chem. Phys. Lett.*, 1977, **51**, 329–332.
- 87 Y. Chen, A. M. Kushner, G. A. Williams and Z. Guan, *Nat. Chem.*, 2012, **4**, 467–472.
- 88 P. Cordier, F. Tournilhac, C. Soulié-Ziakovic and L. Leibler, *Nature*, 2008, **451**, 977–980.
- 89 A. Sánchez-Ferrer, D. Rogez and P. Martinoty, *Macromol. Chem. Phys.*, 2010, **211**, 1712–1721.
- 90 Y. Peng, L. Zhao, C. Yang, Y. Yang, C. Song, Q. Wu, G. Huang and J. Wu, *J. Mater. Chem. A*, 2018, **6**, 19066–19074.
- 91 X. Liu, M. Li, X. Zheng, E. Retulainen and S. Fu, *Materials*, 2018, **11**, 1725.
- 92 A. Matsumoto, M. Kawaharazuka, Y. Takahashi, N. Yoshino, T. Kawai and Y. Kondo, *J. Oleo Sci.*, 2010, **59**, 151–156.
- 93 T. Carofiglio, C. Fregonese, G. J. Mohr, F. Rastrelli and U. Tonellato, *Tetrahedron*, 2006, **62**, 1502–1507.
- 94 Y. Yu, M. Nakano and T. Ikeda, *Nature*, 2003, **425**, 145.
- 95 H. Gan and C. Yi, *Fibers Polym.*, 2015, **16**, 17–22.
- 96 R. Christie, *Colour Chemistry*, The Royal Society of Chemistry, 2001.
- 97 C. Xing, L. Wang, L. Xian, Y. Wang, L. Zhang, K. Xi, Q. Zhang and X. Jia, *Macromol. Chem. Phys.*, 2018, **219**, 1800042.
- 98 M.-Q. Zhu, L. Zhu, J. J. Han, W. Wu, J. K. Hurst and A. D. Q. Li, *J. Am. Chem. Soc.*, 2006, **128**, 4303–4309.
- 99 C. Li and S. Liu, *Chem. Commun.*, 2012, **48**, 3262–3278.
- 100 Q. Chen, Y. Feng, D. Zhang, G. Zhang, Q. Fan, S. Sun and D. Zhu, *Adv. Funct. Mater.*, 2010, **20**, 36–42.



## Review

- 101 C. Li, Y. Zhang, J. Hu, J. Cheng and S. Liu, *Angew. Chem.*, 2010, **122**, 5246–5250.
- 102 G. O'Bryan, B. M. Wong and J. R. McElhanon, *ACS Appl. Mater. Interfaces*, 2010, **2**, 1594–1600.
- 103 F. M. Raymo and S. Giordani, *J. Am. Chem. Soc.*, 2001, **123**, 4651–4652.
- 104 G. R. Gossweiler, G. B. Hewage, G. Soriano, Q. Wang, G. W. Welshofer, X. Zhao and S. L. Craig, *ACS Macro Lett.*, 2014, **3**, 216–219.
- 105 P. Froimowicz, H. Frey and K. Landfester, *Macromol. Rapid Commun.*, 2011, **32**, 468–473.
- 106 J.-F. Xu, Y.-Z. Chen, L.-Z. Wu, C.-H. Tung and Q.-Z. Yang, *Org. Lett.*, 2013, **15**, 6148–6151.
- 107 H. Xie, M. He, X.-Y. Deng, L. Du, C.-J. Fan, K.-K. Yang and Y.-Z. Wang, *ACS Appl. Mater. Interfaces*, 2016, **8**, 9431–9439.
- 108 J. Ling, M. Z. Rong and M. Q. Zhang, *J. Mater. Chem.*, 2011, **21**, 18373–18380.
- 109 C. Salgado, M. P. Arrieta, L. Peponi, M. Fernández-García and D. López, *Macromol. Mater. Eng.*, 2017, **302**, 1600515.
- 110 C. Salgado, M. P. Arrieta, L. Peponi, M. Fernández-García and D. López, *Eur. Polym. J.*, 2017, **93**, 21–32.
- 111 K. Bouchemal, S. Brianchon, E. Perrier, H. Fessi, I. Bonnet and N. Zydowicz, *Int. J. Pharm.*, 2004, **269**, 89–100.
- 112 L. Korchia, C. Bouilhac, V. Lapinte, C. Travelet, R. Borsali and J.-J. Robin, *Polym. Chem.*, 2015, **6**, 6029–6039.
- 113 H. Xie, K.-K. Yang and Y.-Z. Wang, *Mater. Today: Proc.*, 2019, **16**, 1524–1530.
- 114 M. Rubinstein, B. Amit and A. Patchornik, *Tetrahedron Lett.*, 1975, **16**, 1445–1448.
- 115 H. Zhao, E. S. Sterner, E. B. Coughlin and P. Theato, *Macromolecules*, 2012, **45**, 1723–1736.
- 116 S. Wu and H.-J. Butt, *Phys. Chem. Chem. Phys.*, 2017, **19**, 23585–23596.
- 117 C. Decker, *Polym. Int.*, 2002, **51**, 1141–1150.
- 118 A. Ravve, *Light-Associated Reactions of Synthetic Polymers*, 2006, pp. 23–122.
- 119 F. Wang, J. Q. Hu and W. P. Tu, *Prog. Org. Coat.*, 2008, **62**, 245–250.
- 120 P. Occhetta, R. Visone, L. Russo, L. Cipolla, M. Moretti and M. Rasponi, *J. Biomed. Mater. Res., Part A*, 2015, **103**, 2109–2117.
- 121 T. Billiet, E. Gevaert, T. De Schryver, M. Cornelissen and P. Dubruel, *Biomaterials*, 2014, **35**, 49–62.
- 122 A. D. Rouillard, C. M. Berglund, J. Y. Lee, W. J. Polacheck, Y. Tsui, L. J. Bonassar and B. J. Kirby, *Tissue Eng., Part C*, 2010, **17**, 173–179.
- 123 E. A. Papaj, D. J. Mills and S. S. Jamali, *Prog. Org. Coat.*, 2014, **77**, 2086–2090.
- 124 E. S. Džunuzović, S. V. Tasić, B. R. Božić, J. V. Džunuzović, B. M. Dunjić and K. B. Jeremić, *Prog. Org. Coat.*, 2012, **74**, 158–164.
- 125 T. Vermonden, N. A. M. Besseling, M. J. van Steenbergen and W. E. Hennink, *Langmuir*, 2006, **22**, 10180–10184.
- 126 D. Liu, F. Liu, J. He, L. V. J. Lassila and P. K. Vallittu, *J. Mater. Sci.: Mater. Med.*, 2013, **24**, 1595–1603.
- 127 S. Li, J. Xia, Y. Xu, X. Yang, W. Mao and K. Huang, *Carbohydr. Polym.*, 2016, **142**, 250–258.
- 128 Y. Huang, L. Pang, H. Wang, R. Zhong, Z. Zeng and J. Yang, *Prog. Org. Coat.*, 2013, **76**, 654–661.
- 129 Y. Hu, C. Liu, Q. Shang and Y. Zhou, *J. Coat. Technol. Res.*, 2018, **15**, 77–85.
- 130 G. ten Brinke, F. E. Karasz and T. S. Ellis, *Macromolecules*, 1983, **16**, 244–249.
- 131 J. Hector Sandoval and R. B. Wicker, *Rapid Prototyp. J.*, 2006, **12**, 292–303.
- 132 O. Llorente, M. J. Fernández-Berridi, A. González and L. Irusta, *Prog. Org. Coat.*, 2016, **99**, 437–442.
- 133 B. Fernández-d'Arlas and A. Eceiza, *J. Nanopart. Res.*, 2013, **16**, 2166.
- 134 W. Yi, Y. Wang, G. Wang and X. Tao, *Polym. Test.*, 2012, **31**, 677–684.
- 135 J. R. Dios, C. Garcia-Astrain, S. Gonçalves, P. Costa and S. Lanceros-Méndez, *Compos. Sci. Technol.*, 2019, **181**, 107678.
- 136 K. Ke, V. Solouki Bonab, D. Yuan and I. Manas-Zloczower, *Carbon*, 2018, **139**, 52–58.
- 137 Y. Zheng, Y. Li, K. Dai, M. Liu, K. Zhou, G. Zheng, C. Liu and C. Shen, *Composites, Part A*, 2017, **101**, 41–49.
- 138 G. Liao, W. Zhao, Q. Li, Q. Pang and Z. Xu, *Chem. Lett.*, 2017, **46**, 1631–1634.
- 139 H. Zhou, X. Wang, T. Wang, J. Zeng, Z. Yuan, J. Jian, Z. Zhou, L. Zeng and H. Yang, *Eur. Polym. J.*, 2019, **118**, 153–162.
- 140 Z. Yi, J. Ye, N. Kikugawa, T. Kako, S. Ouyang, H. Stuart-Williams, H. Yang, J. Cao, W. Luo, Z. Li, Y. Liu and R. L. Withers, *Nat. Mater.*, 2010, **9**, 559–564.
- 141 S. Wang, D. Li, C. Sun, S. Yang, Y. Guan and H. He, *J. Mol. Catal. A: Chem.*, 2014, **383–384**, 128–136.
- 142 B. Wang, X. Gu, Y. Zhao and Y. Qiang, *Appl. Surf. Sci.*, 2013, **283**, 396–401.
- 143 J. Cao, B. Luo, H. Lin, B. Xu and S. Chen, *J. Hazard. Mater.*, 2012, **217–218**, 107–115.
- 144 M. Rai, A. Yadav and A. Gade, *Biotechnol. Adv.*, 2009, **27**, 76–83.
- 145 Q. L. Feng, J. Wu, G. Q. Chen, F. Z. Cui, T. N. Kim and J. O. Kim, *J. Biomed. Mater. Res.*, 2000, **52**, 662–668.
- 146 R. R. Hardy, *Encycl. Immunol.*, 1998, 943–947.
- 147 J. B. Grimm, L. M. Heckman and L. D. Lavis, *Prog. Mol. Biol. Transl. Sci.*, 2013, **113**, 1–34.
- 148 L. Zhao, W. Li, A. Plog, Y. Xu, G. Buntkowsky, T. Gutmann and K. Zhang, *Phys. Chem. Chem. Phys.*, 2014, **16**, 26322–26329.
- 149 D. P. Nair, N. B. Cramer, M. K. McBride, J. C. Gaipa, R. Shandas and C. N. Bowman, *Polymer*, 2012, **53**, 2429–2434.
- 150 S. J. Ma, S. J. Mannino, N. J. Wagner and C. J. Kloxin, *ACS Macro Lett.*, 2013, **2**, 474–477.
- 151 L. Peng, S. Liu, A. Feng and J. Yuan, *Mol. Pharm.*, 2017, **14**, 2475–2486.
- 152 Y. A. Alemayehu, W.-L. Fan, F. B. Ilhami, C.-W. Chiu, D.-J. Lee and C.-C. Cheng, *Int. J. Mol. Sci.*, 2020, **21**, 4677.

